A co-culture system of macrophages with breast cancer tumoroids to study cell interactions and therapeutic responses

Antonella Raffo Romero, Lydia Ziane Chaouche, Sophie Salome, Nawale Hajjaji, Isabelle Fournier, Michel Salzet, Marie Duhamel

Cell Reports
Methods

Article

A co-culture system of macrophages with breast cancer tumoroids to study cell interactions and therapeutic responses

Graphical abstract

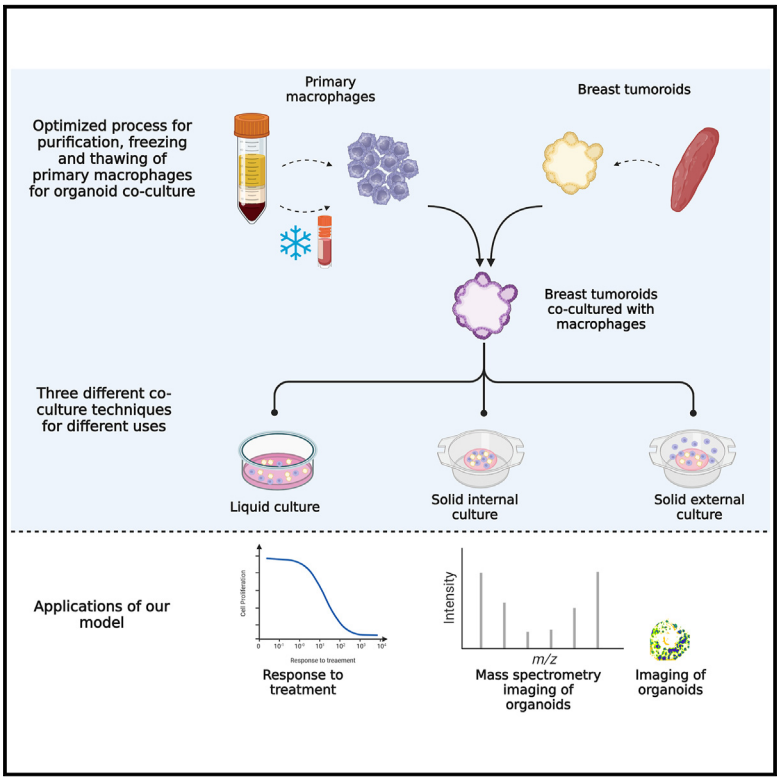

Highlights

- Establishes three optimized breast cancer tumoroid-macrophage co-culture systems
- Demonstrates physio-pathological relevance of the co-culture models
- Co-culture impacts drug response profiles, emphasizing need to enhance model complexity
- These 3D models can be tailored to address varied biological questions

Authors

Antonella Raffo-Romero, Lydia Ziane-Chaouche, Sophie Salomé-Desnoulez, Nawale Hajjaji, Isabelle Fournier, Michel Salzet, Marie Duhamel

Correspondence

michel.salzet@univ-lille.fr (M.S.), marie.duhamel@univ-lille.fr (M.D.)

In brief

3D tumoroids replicate tumor diversity but lack immune cells. Raffo-Romero et al. devise three optimized co-culture methods for human macrophages and breast cancer tumoroids. By tracking the macrophage-tumoroid interactions, they show that macrophages influence tumor molecular profiles and chemotherapy response, emphasizing the need to enhance model complexity for accurate *in vivo* representation.

Raffo-Romero et al., 2024, Cell Reports Methods *4*, 100792
June 17, 2024
https://doi.org/10.1016/j.crmeth.2024.100792

CellPress

Cell Reports Methods

CellPress
OPEN ACCESS

Article

A co-culture system of macrophages with breast cancer tumoroids to study cell interactions and therapeutic responses

Antonella Raffo-Romero,[1,4] Lydia Ziane-Chaouche,[1,4] Sophie Salomé-Desnoulez,[2] Nawale Hajjaji,[1,3] Isabelle Fournier,[1] Michel Salzet,[1,*] and Marie Duhamel[1,5,*]

[1]Université Lille, Inserm, CHU Lille, U1192, Laboratoire Protéomique, Réponse Inflammatoire Et Spectrométrie de Masse (PRISM), Equipe Labellisée Ligue Contre le Cancer, Lille, France

[2]University Lille, CNRS, Inserm, CHU Lille, Institut Pasteur de Lille, US 41 – UAR 2014 – PLBS, F-59000 Lille, France

[3]Breast Cancer Unit, Oscar Lambret Center, Lille, France

[4]These authors contributed equally

[5]Lead contact

*Correspondence: michel.salzet@univ-lille.fr (M.S.), marie.duhamel@univ-lille.fr (M.D.)

https://doi.org/10.1016/j.crmeth.2024.100792

MOTIVATION Cancer research has traditionally relied on 2D cell cultures and xenografts, failing to capture tumor complexity. Organoids, especially tumoroids derived from tumors, offer a promising alternative. However, current 3D models lack crucial immune cells, essential for tumor development and treatment response. Integrating immune cells into tumoroids is crucial to enhance their accuracy. We aimed to establish standardized methods for co-culturing human macrophages with breast cancer tumoroids, optimizing conditions to replicate macrophage-tumor interactions. Our study emphasizes the significance of macrophages in tumoroid drug responses, highlighting the necessity for more complex 3D models.

SUMMARY

3D tumoroids have revolutionized *in vitro*/*ex vivo* cancer biology by recapitulating the complex diversity of tumors. While tumoroids provide new insights into cancer development and treatment response, several limitations remain. As the tumor microenvironment, especially the immune system, strongly influences tumor development, the absence of immune cells in tumoroids may lead to inappropriate conclusions. Macrophages, key players in tumor progression, are particularly challenging to integrate into the tumoroids. In this study, we established three optimized and standardized methods for co-culturing human macrophages with breast cancer tumoroids: a semi-liquid model and two matrix-embedded models tailored for specific applications. We then tracked interactions and macrophage infiltration in these systems using flow cytometry and light sheet microscopy and showed that macrophages influenced not only tumoroid molecular profiles but also chemotherapy response. This underscores the importance of increasing the complexity of 3D models to more accurately reflect *in vivo* conditions.

INTRODUCTION

For decades, cancer research has relied on *in vitro* 2D cell cultures and *in vivo* xenografts. However, both these models fail to capture the complex diversity of tumors. Organoids, self-organizing three-dimensional (3D) structures grown from tissues like tumors,[1] have emerged as a promising alternative. When derived from tumors, these structures are termed tumoroids and have revolutionized *in vitro* cancer biology.[2–5] 3D cell culture offers several advantages over 2D models, including cell-cell interactions, cell-matrix interaction, and spatial organization, which are critical factors influencing cellular behavior and response to therapeutics.[6] Therefore, 3D models can play a pivotal role during preclinical drug development. While tumoroid models offer new insights into cancer development and treatment response, they come with several limitations. Cancer development and treatment response are heavily influenced by the tumor microenvironment (TME), including the surrounding immune system. Consequently, the absence of immune cells in tumoroids can lead to inappropriate treatment responses. Developing more complex tumoroid models is thus imperative.

Efforts have been made to incorporate immune cells into tumoroids for testing cancer immunotherapies and advancing personalized medicine. The most common approach involves

culturing dissociated tumor cells in a Matrigel dome, but this method typically retains only tumor epithelial cells, with stromal cells eliminated during early passages.[7,8] To address this limitation, other tumoroid culture techniques have been explored, such as air-liquid interface (ALI) transwell culture, which provides adequate oxygen supply. Although this method can maintain stromal cell populations, it has been shown to last no longer than 1–2 months.[9] Additionally, the ALI method requires large tumor samples to provide sufficient microenvironmental components, excluding tumor biopsy samples, which are the main source of tissue for tumoroid research. Another strategy involves adding exogenous stromal cell types within the Matrigel dome. The addition of cancer-associated fibroblasts (CAFs) has been carried out using this technique and has revealed different phenotypes of CAFs.[10] The same technique has been used to reconstitute various immune cell types such as T lymphocytes in the presence of anti-PD-L1 antibodies.[11] Tumoroid models have also been used to co-culture natural killer (NK) cells expressing a chimeric antigen receptor (CAR) targeting epidermal growth factor receptor variant III with colorectal cancer organoids to assess CAR tumor-specific cytotoxicity.[12] These immune-supplemented models show promise for immunotherapeutic preclinical testing. The ALI approach preserves the *in vivo* composition of the original tumor, allowing the testing of immunotherapeutics, while the addition of exogenous immune cells to the tumoroids supports long-term culture and in-depth study of cell-cell interactions and the testing of adoptive cell transfer immunotherapies.

Macrophages, the most abundant immune population in the TME, play a pivotal role as tumor-associated macrophages (TAMs),[13] comprising approximately 50% of hematopoietic cells. TAMs are known for their pro-tumorigenic functions, including angiogenesis, invasion, and metastasis promotion, as well as suppression of anti-tumor immune responses and reduction of chemo- and radiotherapy efficacy. Given their significant impact on tumor development, it is crucial to incorporate TAMs into preclinical models. Few studies have described the 3D co-culture of macrophages with tumoroids. In a previous study, the authors have mixed murine TAMs with mouse ovarian cancer cells in a medium containing 2% Matrigel, allowing a direct contact.[14] While this method allows a direct contact between cancer cells and TAMs, the removal of the matrix does not recapitulate the physiological context of the tumor. Despite some attempts at co-culturing macrophages with tumoroids, standardization remains lacking. Optimal culturing conditions are essential to maintain the persistence of immune cells of interest.

In this study, we established three simple, optimized, and standardized methods for co-culturing human macrophages with breast cancer tumoroids. We used semi-liquid culture or Matrigel embedded culture, optimizing macrophage numbers and culture medium to accurately reproduce macrophage-tumor cells interactions. We demonstrated these interactions using two-photon microscopy and mass spectrometry imaging (MSI). Furthermore, we showed that tumoroids exhibit distinct drug responses in the presence of macrophages, highlighting the need to enhance the complexity of current 3D models for better *in vivo* reflection.

RESULTS

Establishment of breast cancer tumoroids, isolation of monocyte-derived macrophages, and optimization of their culture conditions

Prior to initiating macrophage-tumoroid co-cultures, human peripheral blood mononuclear cells (PBMCs) were isolated from blood, and tumoroids were prepared from a breast cancer biopsy (Figure 1A). We used organoids derived from fresh human breast tumor tissue of the luminal subtype, which accounts for 65% of breast cancers.[15] As previously described,[7] the tumor biopsy was mechanically and enzymatically dissociated to obtain single-cell suspensions, which were then plated in Matrigel drops and overlaid with adapted mammary tumoroid culture medium (Figure 1D). Given the limited size of the biopsy, we optimized the protocol to minimize the loss of biological material at each stage. This involved miniaturizing the protocol by reducing all reaction buffer volumes, cutting the biopsy into 1 mm pieces, and performing digestion in a maximum volume of 2 mL. In addition, we used smaller filters coated with a 1% BSA solution for filtration after digestion to prevent cell adhesion. The resulting cells were cultured in Matrigel drops with two expansion media types, namely type 1 and type 2, previously reported in the literature.[16] In some tumoroid cultures, the use of type 2 media (containing hydrocortisone, β-estradiol, and forskolin) resulted in improved growth characteristics. In order to identify the most optimal media type for each donor, newly established tumoroid cultures were grown in both type 1 and type 2 expansion media. The cells were concentrated as much as possible in the Matrigel drop, as we have observed that some subtypes seemed to grow only when there were many cell-cell contacts. We then carefully multiplied the tumoroids according to the culture medium that allowed them to proliferate better, until we had enough for cryopreservation.

On the other hand, PBMCs were isolated using a Ficoll gradient (Figure 1B) and either used directly or cryopreserved for future use (Figure 1C). As working with already differentiated macrophages can complicate the process of co-culturing due to the sensitivity of macrophages to culture conditions, we tried co-culturing tumoroids directly with PBMCs. Attempting to co-culture tumoroids directly with PBMCs to induce monocyte differentiation into macrophages within the tumoroids yielded limited success due to low infiltration (Figures S1A and S1B). Unlike already differentiated macrophages, PBMCs remained on the surface of the matrix and had difficulty penetrating it, as evidenced by vital dye labeling (Figure S1A). This was also demonstrated by labeling the cells with a vital dye, which showed a higher infiltration of already differentiated macrophages within the tumoroids compared to PBMCs (Figure S1B).

Based on these observations, we decided to co-culture tumoroids with already differentiated macrophages for subsequent experiments. Before developing co-culture models, we optimized the culture conditions of macrophages to maximize recovery yield. After purifying PBMCs, monocytes were allowed to adhere to the plate for 2 h before differentiation into macrophages over 7 days in the presence of macrophage colony stimulating factor (M-CSF). Flow cytometry with the CD11b marker and immunofluorescence staining with CD68 confirmed

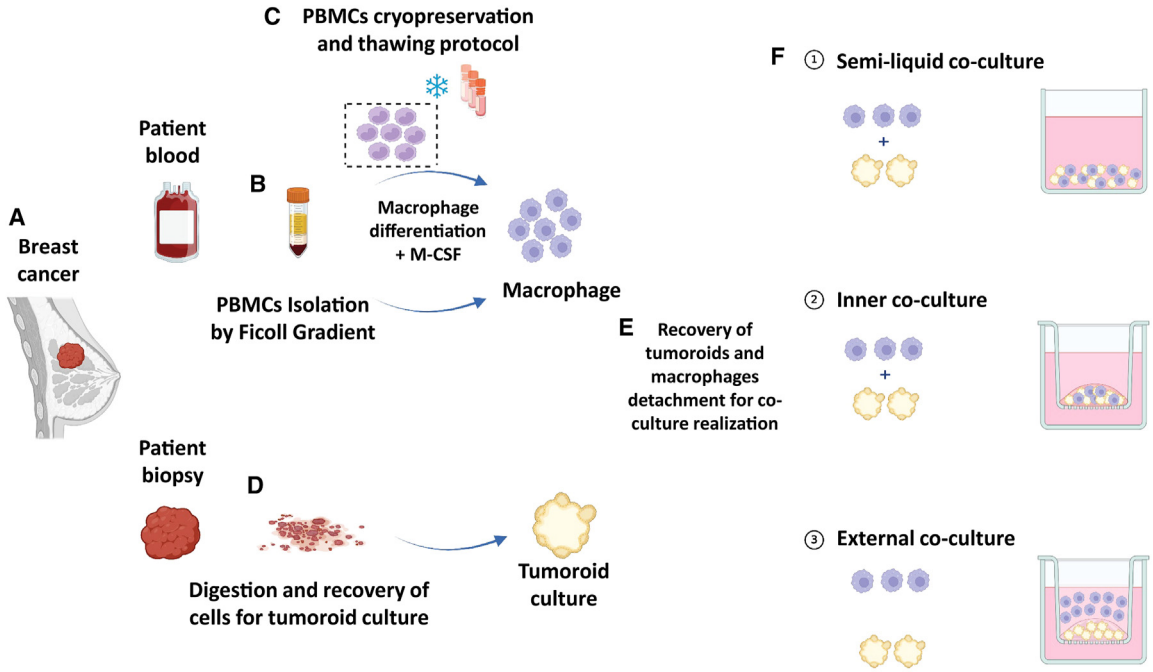

Figure 1. Schematic of co-culture techniques

(A) A biopsy and a blood sample were obtained from patients with different types of breast cancer.

(B) PBMCs were purified from the blood using the Ficoll gradient protocol.

(C) PBMCs were either used directly or frozen. We performed tests to thaw them in the best way and with the best viability. Finally, the fresh or frozen PBMCs were differentiated into macrophages with M-CSF for 7 days. (D) In parallel, the biopsy was minced and gently digested, and the biopsy cells were harvested and placed in culture for the development of breast cancer tumoroids.

(E) For co-culture, the tumoroids were harvested and digested, and the macrophages were harvested.

(F) Three different types of co-culture were performed. 1 was a semi-liquid culture, allowing interactions directly in the liquid. 2 was an internal co-culture where macrophages and tumoroids were mixed and placed in the matrix in a transwell, allowing direct contact in a viscous matrix. 3 was an external co-culture where the macrophages were on top and the tumoroids were in the matrix in the transwell.

a macrophage purity of over 97% after 7 days (Figure 2A, S2A and S2B). To overcome limitations of freshly isolated PBMCs, we developed a protocol for cryopreservation and recovery of monocytes after thawing (Figure 2B). In addition, this step will allow the future development of co-culture models with both macrophages and tumor cells from the same patient. In this way, when the tumoroids are ready for co-culture, the PBMCs can be thawed. This avoids any mismatch between the tumoroid and macrophage cultures, as tumoroid growth takes longer than macrophage differentiation. Cryopreserved PBMCs were thawed and then washed prior to plating. We compared different wash media, and finally three were found to work correctly: RPMI with 0.1% EDTA without fetal bovine serum (FBS), with 1% FBS, and with 20% FBS(Figure S3A). Among the three, we did not see important visible differences that would justify the use of 20% FBS, so we decided to continue with two wash media, i.e., RPMI with 0.1% EDTA without FBSor with 1% FBS. The two wash media were tested after recovery of macrophages. The addition of serum to the wash medium is a key factor in achieving good viability after freezing, which is 1.6 times higher than with the wash medium without serum (Figure 2D). We then optimized the culture of thawed PBMCs and their differentiation into macrophages to achieve maximum recovery. We first tried to differentiate them by using the conventional method of plating them in serum-free medium for 2 h at 37°C and cultivating them for 7 days in complete classical medium with M-CSF. Unfortunately, this approach produced a few differentiated cells and a significant number of dead cells (Figure S3B). We therefore tried a medium specifically designed for efficient monocyte attachment selection, called monocyte attachment medium (PromoCell), and although this method showed a small improvement, the results were still not optimal with only a few differentiated cells (Figure S3B). Therefore, we decided to skip the 2-h culture step, which allows monocytes to adhere to the plate, and directly induce monocyte differentiation into macrophages. In this modified approach, we cultured PBMCs directly in complete medium with M-CSF for 7 days, replacing half of the medium with fresh medium after 48 h, which significantly improved the yield (Figure S3C). Two culture media were tested, the classical complete culture medium and an optimized X-VIVO15 macrophage differentiation medium (Lonza), both containing M-CSF. This optimized culture medium helped to obtain healthier macrophages after thawing, with the typical elongated morphology of differentiated macrophages, compared to the classical RPMI medium used for routine macrophage culture (Figure S3C). After 7 days of differentiation, the macrophages had the same elongated morphology as those derived from freshly isolated monocytes and expressed the macrophage marker CD68 (Figure 2C). The

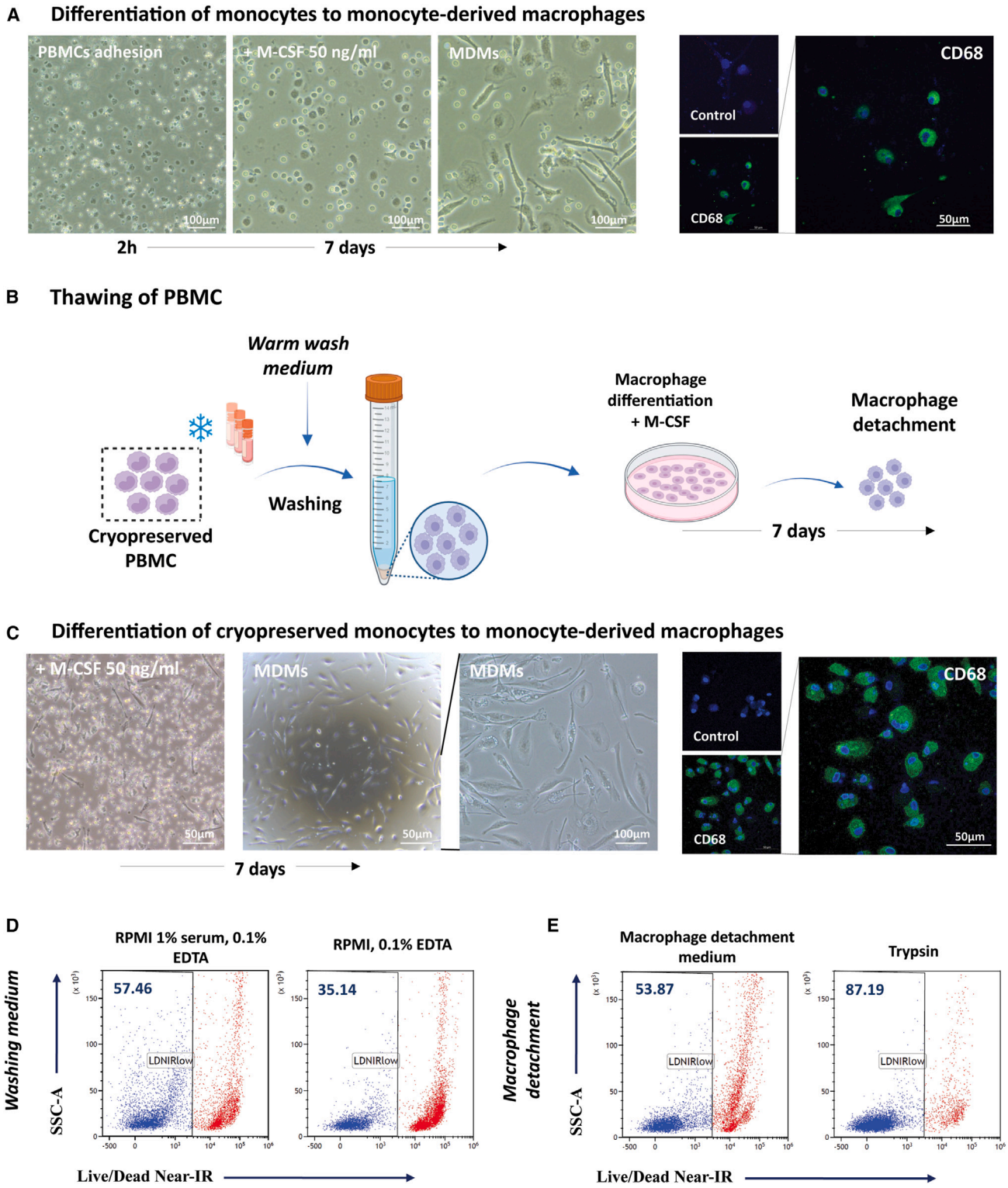

Figure 2. Purification, freezing, and thawing of PBMCs from blood

(A) PBMCs were purified by a classical Ficoll gradient followed by differentiation into macrophages using M-CSF for 7 days. Representative immunofluorescence images depict CD68 staining after differentiation. A control image was included without the primary antibody.

(B) Experimental procedure outlining the thawing of PBMCs and their differentiation into macrophages.

(legend continued on next page)

final step before performing the co-culture was to optimize the macrophage detachment protocol. In fact, macrophages are very sticky cells that are difficult to detach. We developed a protocol that allowed us to reduce the loss while maintaining good macrophage viability, as only 5%–10% of the initially plated cells differentiate into macrophages and can potentially be recovered. Two detachment solutions were tested: trypsin and a commercial reagent called macrophage detachment solution. The commercial solution is non-enzymatic and optimized for gentle detachment of strongly adherent macrophages. The main difference between the two methods, apart from the solution used, was their length. The trypsin digestion took 2 times 10 min, while the macrophage detachment solution protocol took 1 h and a half. From the same number of initially plated PBMCs (10 million), we recovered approximately 1 million macrophages using the trypsin method and 100,000 macrophages using the macrophage detachment solution method (Figure S2C). More importantly, macrophage viability after detachment was also higher using the trypsin protocol, with approximately 87% of cells being viable, which is 1.6 times higher than using the macrophage detachment solution (Figure 2E).

In summary, we established optimal culture conditions for primary human macrophages to initiate co-cultures with tumoroids.

Co-culture establishment and comparison of the three setups

We have established three different co-culture systems that serve various purposes (Figure 1F). The first system is a semi-liquid co-culture model facilitating direct interactions between macrophages and tumoroids, containing only 2% Matrigel in the medium and performed in a non-adherent plate. This model facilitates 3D imaging of the whole model and viability testing, as tumoroids are more readily recoverable. The other two models are solid-state co-culture systems where cells are embedded in a Matrigel matrix. The primary difference between the two models lies in the placement of macrophages: either directly embedded in the matrix with the tumoroids (inner co-culture) or outside the matrix in the culture medium (external co-culture). These models enable the replication of macrophage-tumoroid interactions in a more complex physical environment and allow for the tracking of macrophage infiltration into the matrix, specifically in the external co-culture system. From a technical perspective, they are user-friendly when sections are needed for imaging techniques (e.g., microscopy and MSI).

For the establishment of the three models, we recovered tumoroids from Matrigel drops by trypsinization and harvested macrophages as described previously. To best mimic *in vivo* conditions, we set the percentage of macrophages and tumor cells to 30% and 70%, respectively.

We first characterized the degree of macrophage infiltration within the tumoroids in each co-culture type using various techniques. To track macrophages over time during culture, we labeled them with the vital dye CytoTell green. After 1 day in culture, macrophages were observed and distributed around the tumoroids, as indicated by white arrows (Figure 3A). As expected, macrophages are scarcely visible in the external co-culture, as they had not yet penetrated the Matrigel matrix. By day 3 of culture, macrophages were visible in all three setups and began to aggregate around the tumoroids, particularly in the semi-liquid co-culture where interactions were not constrained by the matrix (Figure 3B). Macrophages successfully invaded the matrix in the external co-culture system (Figures 3B and S1C). By day 7 of culture, clear infiltration and interactions of macrophages within the tumoroids were observed, regardless of the setup (Figure 3C). We then used flow cytometry to quantify the percentage of macrophage infiltration in the three co-culture systems. The results indicated that 17.1%, 9.8%, and 26% of macrophages labeled with the anti-CD11b marker were present in the semi-liquid, external, and inner co-cultures, respectively (Figures 3D and S4A). These levels of macrophage infiltration were reproducible (Figure 3E). The lower level of macrophage infiltration observed in the external co-culture was normal, as macrophages had to cross a physical barrier. This setup may be valuable for comparing differences in macrophage attraction in different tumor types or treatment conditions. The higher macrophage infiltration capacity was obtained with the semi-liquid and inner co-culture systems, although a slight difference was observed between the two systems.

To further characterize the three systems, we established an immunofluorescence protocol of the intact 3D structures through transparization (Figure 4A). The tumoroids were harvested 10 days after the start of co-culture and placed in a Lab-Tek chamber for all steps of the immunofluorescence protocol. The only difference among the three setups was that the semi-liquid, matrix-free tumoroids were adhered to the Lab-Tek, which was first coated with poly-D-lysine. The other two models, embedded in the matrix, were transferred directly to the Lab-Tek. We intentionally left the matrix in place throughout the protocol to minimize the risk of damaging the tumoroids. After fixation, permeabilization, and blocking, tumoroids were incubated with the anti-CD68 antibody to label macrophages. In some cases, macrophages were pre-labeled with CytoTell green before co-culture to eliminate the need for additional permeabilization, blocking, and antibody incubation steps. Finally, the tumoroids were made transparent using formamide and polyethylene glycol to enhance the fluorescence by improving light scattering. This transparization step was critical because without it, fluorescence decreased as we penetrated deeper into the tumoroids. During the protocol's development, we demonstrated that without transparization, background noise in the images obscured the specific label, especially in embedded matrix conditions (Figure S5). Light-sheet fluorescence microscopy was then performed using this optimized protocol to analyze macrophage infiltration within the tumoroids accurately. Macrophages were either labeled with CytoTell

(C) Thawed PBMCs were differentiated into macrophages with M-CSF for 7 days. Representative immunofluorescence images illustrate CD68 staining after differentiation. A control image was included without the primary antibody.
(D) Flow cytometry results comparing the cell viability of macrophages after using two different post-thaw wash media.
(E) Flow cytometry results comparing the viability of macrophages after detachment from the plate using two different detachment media.

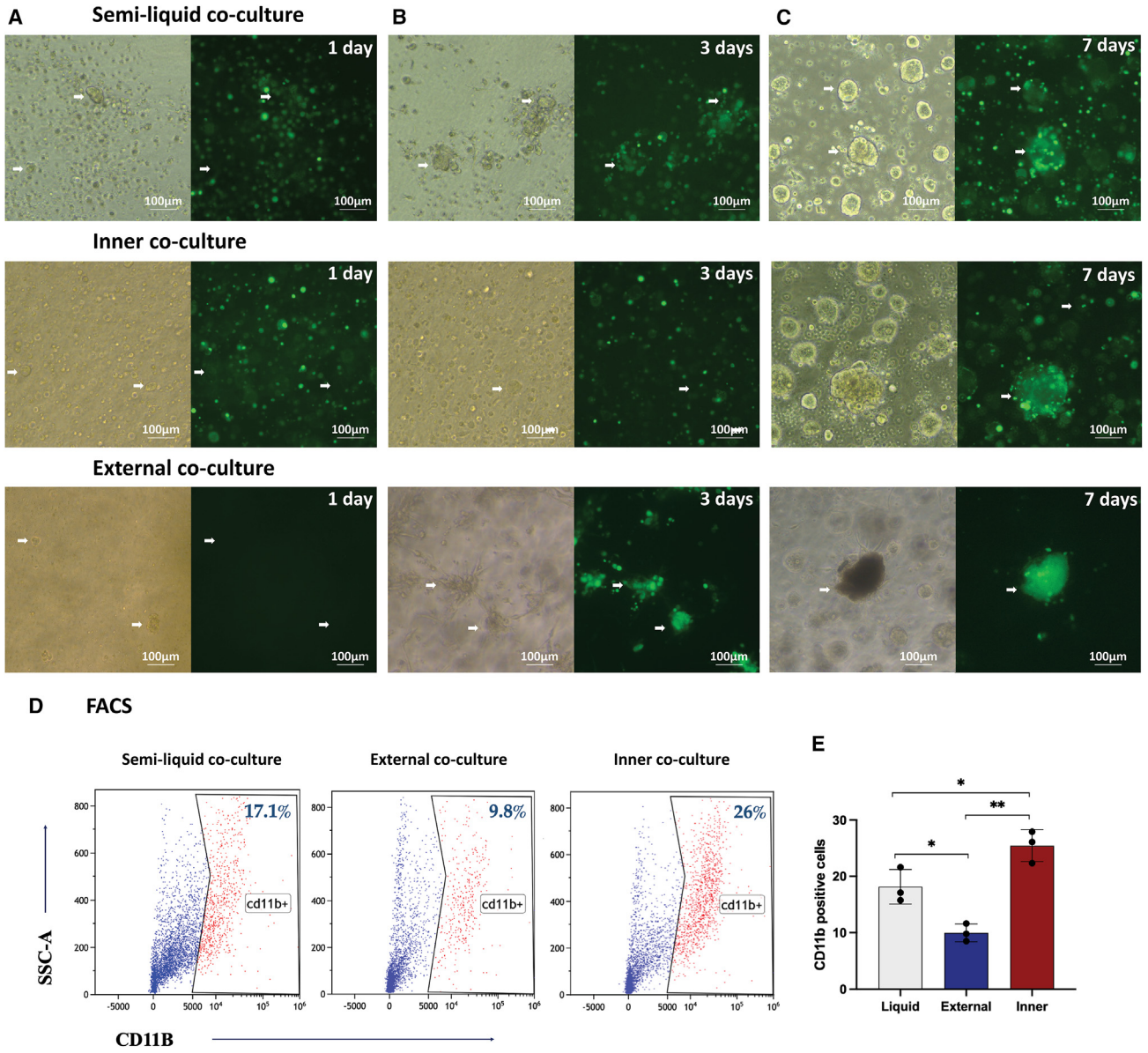

Figure 3. Establishment of the 3 co-culture models

Macrophages were labeled with CytoTell green vital dye and followed during cell culture in each of the three models after 1 day (A), 3 days, (B) and 7 days (C).
(D) Histograms of a representative flow cytometry experiment showing the percentage of CD11b-positive cells by the type of co-culture model.
(E) Bar graph showing the percentage of CD11b+ cells in triplicate by type of co-culture model. Data are expressed as the percentage of CD11b+ cells, error bars are SEM, $n = 3$ independent flow cytometry experiments. Significance was calculated by two-tailed paired t test. $^{*}p < 0.05$, $^{**}p < 0.01$, $^{***}p < 0.001$.

green (Figure 4B) or stained with the anti-CD68 antibody (Figure 4C). The images revealed a higher infiltration of macrophages within the tumoroids for the semi-liquid and inner co-culture setups, consistent with previous observations. In the semi-liquid system, intra-tumoroid macrophage infiltration was evident, whether using CytoTell labeling (Figure 4B) or antibody staining (Figure 4C). Additionally, Video S1 depicted precise macrophage infiltration in 3D within a semi-liquid tumoroid. In the inner co-culture, macrophage interactions with tumoroids were observed, albeit more in the periphery. Finally, in the external co-culture, macrophages penetrated the matrix and made contact with tumoroids.

In summary, the three setups facilitate the study of macrophage-tumoroid interactions to address various biological questions.

Characterization of macrophages in tumoroid-macrophage co-culture

To understand the phenotype acquired by macrophages following co-culture with tumoroids, we conducted a proteomic

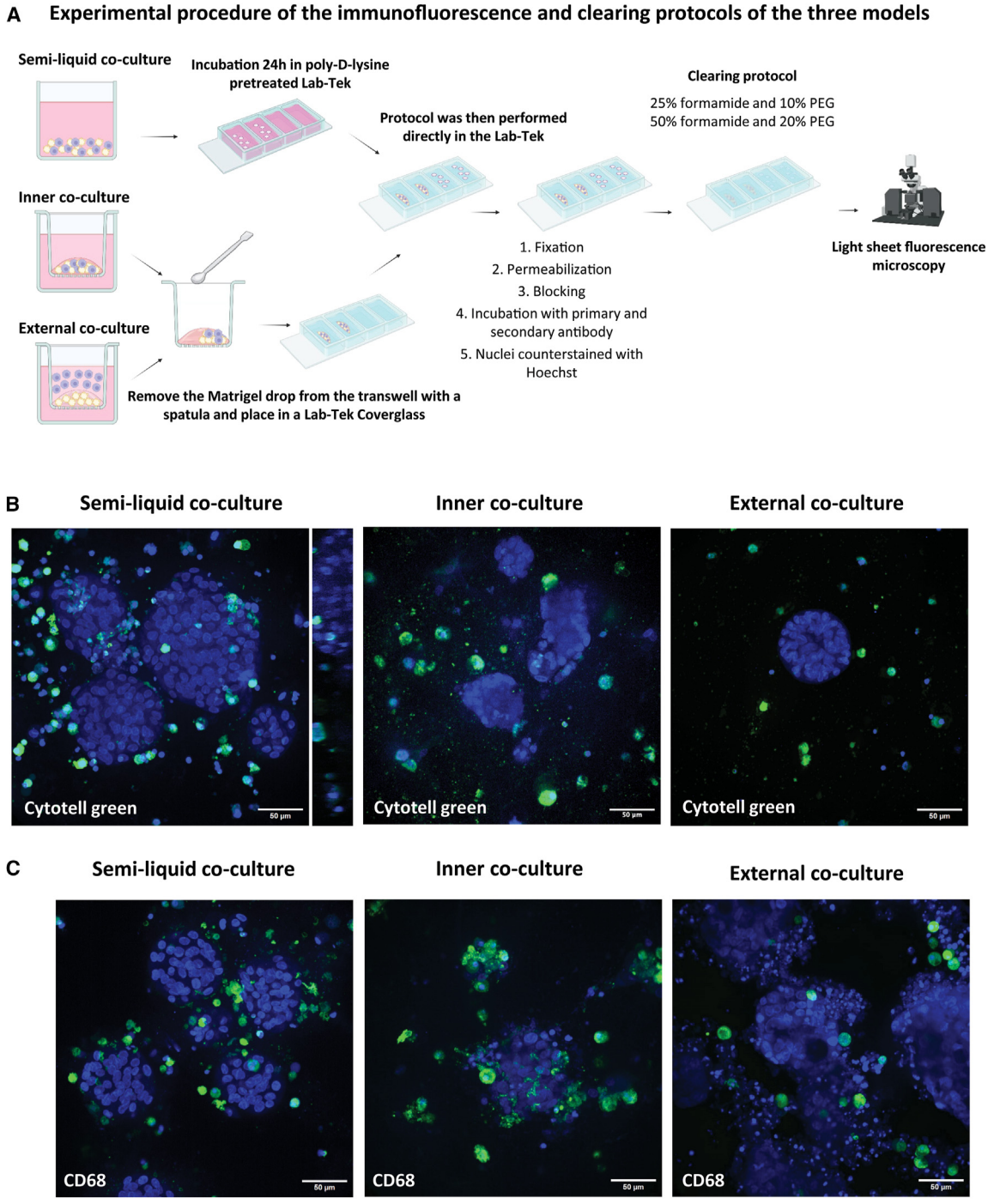

Figure 4. Light-sheet microscopy of transparized tumoroids to characterize macrophage infiltration in the three setups

(A) Illustration of the experimental procedure of the immunofluorescence and clearing protocol of the three models.

(B) Representative light-sheet microscopy images of the tumoroids with CytoTell green-stained macrophages in the three models.

(C) Representative light-sheet microscopy images of the tumoroids with CD68-labeled macrophages (green) in the three models.

study comparing the proteomic profile of macrophages cultured alone versus in co-culture with tumoroids. Liquid co-culture models were employed, and macrophage sorting was conducted via flow cytometry after digesting both the macrophages alone and in co-culture models. The results revealed that approximately 17% of proteins exhibited differential expression between the control macrophages and co-cultured macrophages, either showing overexpression or underexpression,

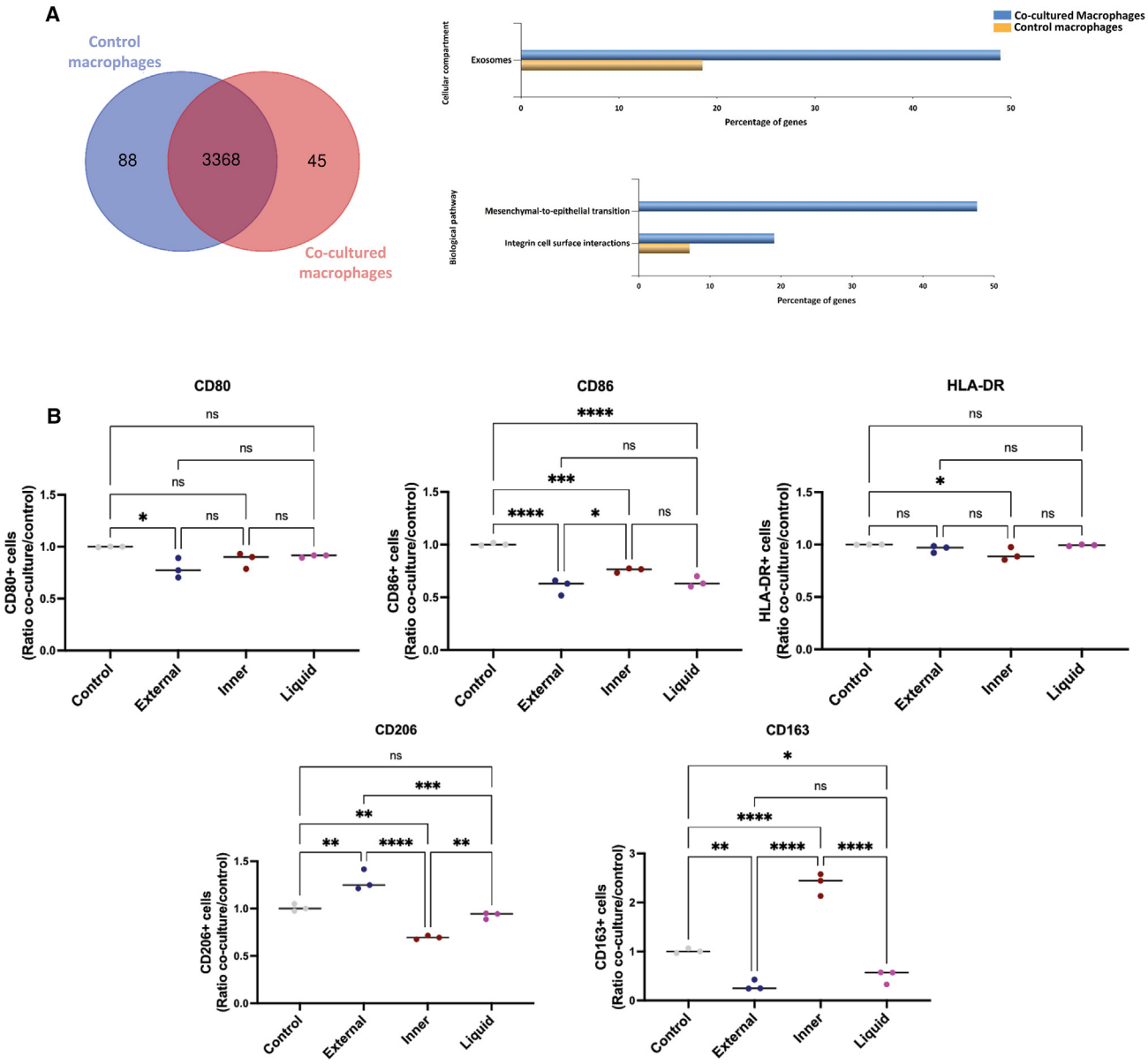

Figure 5. Characterization of macrophages following co-culture with tumoroids in our model

(A) Proteomic analysis comparing control macrophages with macrophages after co-culture with tumoroids. A Venn diagram was used to illustrate specific proteins present in control samples versus those found in macrophages. Furthermore, cellular components and biological pathways associated with the specific identified proteins in co-cultured macrophages versus control were analyzed using FunRich.

(B) Macrophage phenotyping in the three co-cultured models of tumoroids. The co-culture models were first double-digested to obtain single cells, and then labeled with: CD11b BV605, CD80 Pe-Cy5, CD86 BV786, HLA-DR Pe-Cy7, CD206 PE, and CD163 BV421 (BD Biosciences). Cells were gated on lived CD11b+. Macrophages co-cultured in the external, inner, and liquid setups were compared to control macrophages (control), which were not cultured with tumoroids. The results depict the ratio of marker-positive cells in co-culture relative to control. Error bars are SEM; $n = 3$ independent flow cytometry experiments. Significance was calculated by t-test with multiple comparisons. ****p <0.0001; ***p <0.001; **p <0.01; *p <0.05; ns, not significant.

and only about 2% of proteins were found to be specific to both conditions (Figure 5A and S6; Table S1). Regarding the overexpressed proteins when comparing macrophages cultured with tumoroids versus control macrophages, macrophages in co-culture exhibited an increase in molecular and biological functions related to metabolism, energy, transport, and catalytic activities (Figures S6A and S6B). This indicates a metabolic alteration post-culture, consistent with the known reprogramming of energy metabolism in macrophages upon tumor contact,[17] and also represents one of the cancer hallmarks introduced in 2022, constituting a fundamental component of the primary cancer axes.[18] Furthermore, analysis of specific macrophage

proteins revealed an upregulation of proteins involved in exosomes in macrophages in co-culture with tumoroids, as described for TAMs (Figure 5A). Studies have shown that TAMs lead to the secretion of high levels of exosomes, which has a direct impact on tumor development.[19] Additionally, analysis of macrophage-specific proteins indicated an elevation in proteins associated with the mesenchymal-to-epithelial transition and integrin interactions with the cell surface (Figure 5A). It has been demonstrated that conditioned medium from M2 macrophages significantly enhances epithelial-mesenchymal transition. Moreover, it has been demonstrated that integrin-mediated adhesion of macrophages promotes dissemination, particularly in triple-negative breast cancer.[20,21] Both have a direct relationship with poor prognosis and are studied in highly aggressive cancers. Additionally, some known TAM markers were more expressed in co-cultured macrophages such as MAOA, FCGR2B, and LGALS3BP[22,23] (Table S1).

All these results support the notion that macrophages transition to a TAM-like phenotype upon interaction with tumoroids in our model. Additionally, despite insights gained from the proteomic profile suggesting that macrophages may adopt a phenotype associated with M2 or TAMs following co-culture with tumoroids, further investigation was necessary to elucidate macrophage phenotype and explore potential variations among the three culture models. Therefore, we conducted a phenotypic analysis of macrophages using flow cytometry in each model after digestion. We analyzed the expression of pro-inflammatory markers (CD80, CD86, and HLA-DR) as well as anti-inflammatory markers (CD206 and CD163) in both control macrophages and those co-cultured within the three setups (Figure 5B and S4B). While the differences observed were not statistically significant, there was a trend indicating fewer $CD80^{+}$ and HLA-DR+ macrophages in the three co-culture conditions. Similarly, there were statistically fewer $CD86^{+}$ macrophages in the three co-cultured conditions. Notably, there was a higher prevalence of CD206+ macrophages in the external co-culture and an increased presence of CD163+ macrophages in the inner co-culture. The percentage of cells expressing pro-inflammatory markers across the three co-culture setups was similar and lower than in the control, suggesting a tendency toward a TAM phenotype. Conversely, more pronounced differences were observed in the expression of anti-inflammatory markers, particularly in the inner and external setups. This suggests that the presence of the matrix may facilitate a higher differentiation into TAMs.[24]

Molecular profiling of tumoroids in the presence or absence of macrophages using MSI

Next, to evaluate the impact of macrophages on the molecular profile of tumoroids, we conducted spatially resolved lipidomic studies using MSI to assess the lipid signatures of tumoroids cultured with or without macrophages (inner co-culture or external co-culture). The Matrigel drops containing the tumoroids were collected fresh and left intact before being embedded in gelatin for cryosectioning at 16 μm on ITO glass slides (Figure 6A). Gelatin, with a consistency similar to Matrigel, facilitated the embedding and sectioning of tumoroids. However, the yellowish transparency of the gelatin made it challenging to distinguish the tumoroids during sectioning. To ensure that we were in the right area, we stained every 4 to 5 sections with toluidine blue until the tumoroids were identified (Figure S7A). Matrix deposition was achieved by sublimating 2,5-dihydroxybenzoic acid onto the slide. Matrix-associated laser desorption/ionization (MALDI) imaging of the sublimated tumoroid sections was then performed using a RapifleX MALDI-TOF/TOF system equipped with a smartbeam 3D laser in positive ionization mode at 10 μm resolution due to the small size of the tumoroids. The spectra data obtained from the spatially resolved lipidomic analysis were processed using SCiLS software, which conducts molecular segmentation of the spectra (Figures S7B and S7D). Segmentation is an unsupervised multivariate statistical analysis that categorizes image pixels based on similarities or differences in their mass spectra. This facilitates the detection of potential molecular differences in the lipidomic profiles of tumoroids with and without macrophages. To correlate the MSI images with the observed tumoroid structures, histological hematoxylin and eosin (H&E) staining of the tumoroid sections was performed after MALDI imaging (Figure S7C). Histological H&E staining after MSI revealed the position of the tumoroids, confirming that the red color of the segmentation map in the images corresponded to the signal of the matrix. Additionally, the SCiLS segmentation results showed that tumoroids cultured without macrophages exhibited a mostly similar and molecularly homogenous profile, indicated by a predominant blue molecular region in most tumoroids. In contrast, tumoroids cultured with macrophages (inner co-culture or external co-culture) showed a more heterogeneous lipid profile, with the presence of blue and green regions (Figure 6B and S7B). Moreover, a signal found around the tumoroids was significantly higher in the co-cultured tumoroid conditions (orange region) than in the control tumoroids, indicating the influence of macrophages in the co-culture models. To identify characteristic peaks associated with the presence of macrophages in the co-culture, we conducted an automated search of the most abundant peaks in the co-cultured models compared to the control ones. Two lipids of m/z 584.449 and 601.454 were more abundant in the co-cultured models (Figure 6C). Other characteristic lipids, mostly in the 500–600 m/z range, likely belong to the ceramide and lysophospholipid classes (Figure S7E). The majority of the characteristic lipids are in the 500–600 m/z range and are most likely to belong to the ceramide and lysophospholipid classes. Notably, these peaks show higher abundance in the co-culture models, particularly in the inner co-culture (Figures 6C, and S7E). This result could be explained by our previous observations, i.e., macrophages were more likely to infiltrate the tumoroids cultured in the inner co-culture condition. These findings suggest that the lipidomic profile of tumoroids is influenced by the presence of macrophages in both models, leading to a more heterogeneous tumoroid profile. Additionally, we also confirmed that these peaks were not solely attributable to macrophages themselves by analyzing the lipid profile of macrophages alone (Figure S7E). Notably, two characteristic peaks showed an association with macrophages, displaying higher abundance in both macrophages alone and co-cultured tumoroids (Figure S7F). This

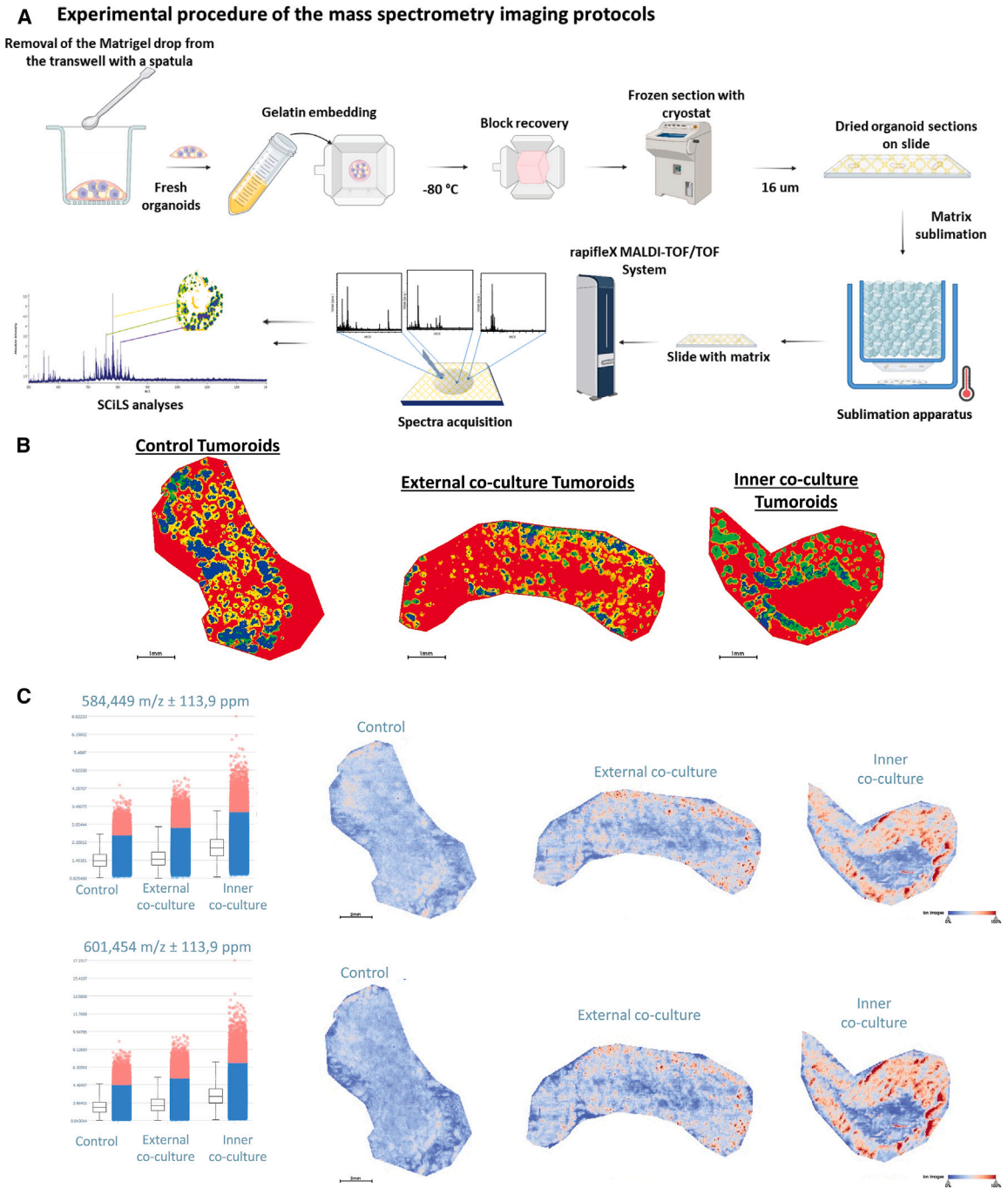

Figure 6. High spatial resolution MALDI-MSI to characterize the molecular profiles of tumoroids cultured with and without macrophages

(A) General workflow for preparation of tumoroids and deposition of sublimated matrix for MALDI-MSI imaging of lipids. Mass spectra were acquired in positive ion mode in a 10 × 10 μm raster using MALDI-ToF.

(B) Global segmentation maps of tumoroids cultured with and without macrophages after MALDI-MSI analysis. Colors represent molecularly distinct regions as shown in the corresponding dendrogram (Figure S6B).

(C) Boxplot of the abundance of characteristic peaks in tumoroids cultured with and without macrophages, together with the localization of these peaks in the mass spectrometry images of the tumoroids. Boxplot indicates median, and whiskers indicate the extrema (minima and maxima values). The box extends from the 25th to the 75th percentiles.

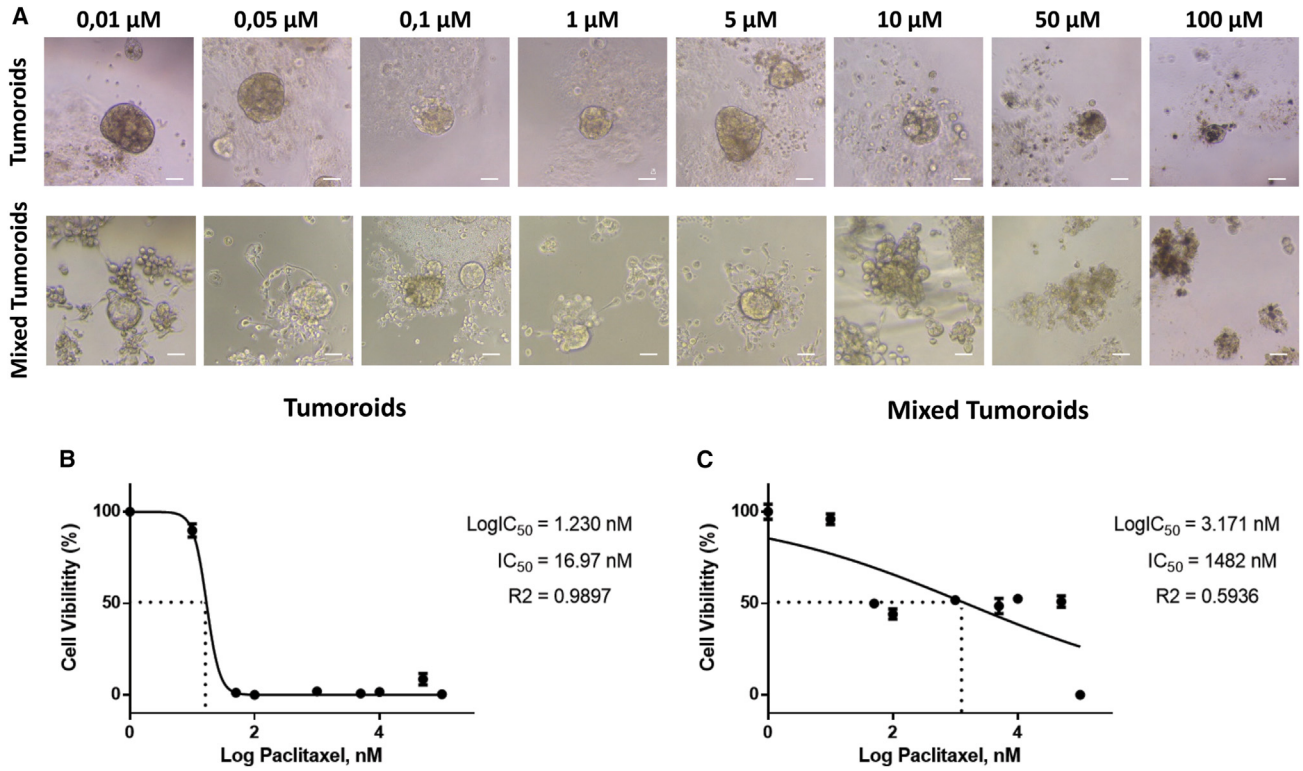

Figure 7. Macrophages influence tumoroid treatment response

Drug response of human tumoroids with and without macrophages to paclitaxel.

(A) Representative bright-field images showing the morphology of the three types of tumoroids after 7 days treatment with paclitaxel at different concentrations. The scale bar (100 µm) is indicated.

(B, C) Quantification of tumoroid viability after paclitaxel treatment. Drug response was compared between tumoroids without (B) and with macrophages (C). Data are mean ± SD. Different drug concentrations were used and compared with untreated tumoroids. Data are mean ± SD (n = 3 per drug concentration).

could have potential implications for the response of tumoroids to treatment, given their diverse and heterogeneous nature after co-culture.

Impact of macrophages on the response of tumoroids to chemotherapy

To assess the impact of macrophages on treatment response, we employed the CellTiter-Glo3D assay in semi-liquid tumoroids. After 3 days in culture, tumoroids co-cultured with or without macrophages were subjected to increasing concentrations of paclitaxel for 7 days. Some tumoroids were treated with escalating concentrations of DMSO as a control, and the viability results were standardized against these controls (in the presence or absence of macrophages). The half-maximal inhibitory concentration (IC_{50}) value of tumoroids was determined using the dose-response curve for nine different concentrations of paclitaxel, ranging from 0.01 to 100 µM. Tumoroids co-cultured with or without macrophages exhibited distinct growth trends (Figure 7A). A decrease in size was observed in tumoroids exposed to high drug concentrations and in the absence of macrophages. The presence of macrophages appeared to protect tumoroids, as larger tumoroids were still observed, albeit slightly disorganized. These observations were supported by the dose-response curves (Figures 7B and 7C). Specifically, the IC_{50} of tumoroids cultured in the absence of macrophages was approximately 17 nM of paclitaxel (Figure 7B). Conversely, macrophages seemed to shield tumoroids from the toxic effects of paclitaxel. Although a decrease in growth was observed from 1 µM compared to the control, tumoroid viability tended to plateau at around 50% regardless of the concentration of the drug used (Figure 7C, with an estimated IC_{50} of 1,482 nM). The protective effect of macrophages against paclitaxel is well established,[25] and our tumoroid model reaffirms this, underscoring the importance of incorporating elements of the TME to accurately predict patient response.

DISCUSSION

A major limitation of *in vitro* 3D cancer models is the absence of immune cells, which play multiple roles in tumor growth. Here, we describe a method to recapitulate macrophage infiltration into the TME by co-culturing breast cancer tumoroids and primary macrophages *in vitro*. Such complex models allow the study of macrophage functions in tumor growth and resistance, as well as therapeutic testing, including macrophage-targeting immunotherapies, unlike existing cancer tumoroid models containing only tumor cells.[3,26] To recapitulate the immune compartment in tumoroids, there are generally two main approaches.

The first involves maintaining the original population of immune cells from the tumor fragment when the tumoroids are cultured.[9] However, immune cell populations are eventually not sustained as the culture progresses due to inappropriate culture conditions favoring tumor cells. Additionally, although autologous co-culture is ideal, the availability of a significant amount of tissue poses a major limitation. The second approach involves reconstituting the immune cell compartment in tumoroid models from blood PBMCs. This has been done for T cells[27–29] with a first step of tumor-reactive T cell generation from co-culture of autologous tumor organoids and peripheral blood lymphocytes. These models have been used to test different types of immunotherapeutic options, from immune checkpoint inhibitors[30] to CAR cell therapies.[12] The latter approach supports long-term culture and is particularly suited to a wide range of applications, such as immunotherapeutic testing or the study of cell-cell interactions. However, since macrophages are the main immune cells in the TME and regulate many pro-tumor functions, including conditioning the TME in an immunosuppressive manner and modulating the immunotherapeutic responses, it is necessary to include them in 3D tumoroid models to best mimic the *in vivo* response. A major challenge in developing co-culture models is the medium, which must be optimal for both tumoroids and immune cells. Tumoroids are cultured in a complex medium containing specific factors required for their growth. While some studies have shown that some factors of the tumoroid media are not suitable for NK or T cell culture, such as nicotinamide,[12,31] we observed a good persistence of macrophages in the complete tumoroid media. In contrast, we only added M-CSF, which allows macrophages to survive and differentiate. Another difficulty may be the density of the matrix, which can be a barrier to good immune cell infiltration. For this reason, most co-cultured tumoroids are grown in the absence of a matrix or with a low percentage of a matrix in the medium.[27,28,31] However, the extracellular matrix is a major component of the TME. Culturing immune cells without extracellular matrix may lead to over-interpretation of the immune cells' immunotherapeutic responses, as cell-cell interactions are favored in this setup and therefore do not recapitulate the solid tumor context. We have therefore developed two models in which tumoroids are grown in an extracellular matrix. Macrophages were added either directly into the matrix or outside the matrix. In these setups, we have shown that macrophages can be efficiently cultured in an extracellular matrix without compromising their mobility to invade tumoroid structures. Interestingly, we have shown that macrophages can penetrate the matrix even when cultured outside it. It can therefore be used to study how tumor cells attract macrophages and the factors that influence this. In fact, the infiltration of macrophages varies from one cancer subtype to another or even from one patient to another. For example, in breast cancer, higher macrophage infiltration has been observed in more aggressive subtypes.[23] Although the matrix plays a key role, we have also developed a matrix-reduced model that can be used for co-culturing with cells for which the matrix can affect their growth or infiltration, such as T cells. Furthermore, we have demonstrated that macrophages in co-culture with tumoroids in all three setups adopt a TAM phenotype, mirroring observations *in vivo*. The advantages of adding macrophages to tumoroid cultures were further demonstrated through MSI, revealing alterations in lipid profile and increased molecular heterogeneity upon macrophage addition. Elevated levels of ceramides and lysophospholipids, both known to influence macrophage polarization,[32,33] were observed in co-cultured tumoroid models. This heightened lipid complexity could indirectly promote pro-tumor effects and therapeutic resistance, as evidenced by previous studies demonstrating the role of these lipids in driving chemotherapeutic resistance.[34,35] Finally, to underscore the importance of incorporating macrophages into tumoroid cultures, we conducted drug response assays. Notably, macrophages have been shown to impact the response to anti-cancer therapies,[36] including paclitaxel.[25,37] We successfully recapitulated paclitaxel resistance in our co-culture models, reaffirming the necessity of macrophage inclusion in 3D tumoroid models to enhance their relevance as avatars of tumor therapeutic response.

In conclusion, the co-culture models we have developed represent a significant advancement in cancer research. They offer a more nuanced and physiologically relevant platform for studying the interactions between tumor cells and the immune system, particularly macrophages. This research deepens our understanding of the TME and holds promise for facilitating more effective investigations into new cancer treatments.

Limitations of the study

In our co-culture models, primary macrophages were used alongside tumoroids, which originate from tumors and thus contain primary tumor cells. However, as is typical with studies involving primary cells, inherent variations among donors are inevitable. While this poses a limitation, it is not unique to our models but rather a common challenge across research employing primary cells. Additionally, the potential discrepancies between patient-derived tumoroids cannot be disregarded, given the observed variations among tumor subtypes and grades. This observation is in line with clinical findings concerning macrophages and is indeed intriguing. Therefore, further investigation is warranted and will be addressed in subsequent studies. Consequently, the inter-patient variability observed in both macrophages and tumoroids stands as a primary limitation of our research.

STAR★METHODS

Detailed methods are provided in the online version of this paper and include the following:

- KEY RESOURCES TABLE
- RESOURCE AVAILABILITY
  - Lead contact
  - Materials availability
  - Data and code availability
- EXPERIMENTAL MODEL AND STUDY PARTICIPANT DETAILS
  - Human patients' tissue collection
  - Purification of blood PBMCs
- METHOD DETAILS
  - Tissue processing
  - Tumoroid culture
  - Isolation of PBMCs from blood
  - PBMC thawing
  - Macrophage recovery
  - Tumoroid and macrophage co-culture models

- Cytotell cell labeling
- Immunofluorescence of macrophages
- Immunofluorescence of macrophages in the 3D co-culture tumoroid models
- Flow cytometry of macrophages and tumoroids
- Cell sorting by flow cytometry after co-culture
- Total protein extraction
- Shotgun proteomics
- LC-MS/MS analysis
- MALDI mass spectrometry imaging of co-cultured tumoroids (MALDI-MSI)
- Tumoroid response to paclitaxel
- Quantification and statistical analysis

SUPPLEMENTAL INFORMATION

Supplemental information can be found online at https://doi.org/10.1016/j.crmeth.2024.100792.

ACKNOWLEDGMENTS

This work was supported by the ITMO Cancer Aviesan grant entitled "Optimisation de la règle des 3R" and by the allocation dedicated to the team of the "Ligue Contre le Cancer." We thank Nathalie Jouy and Emilie Floquet from the US 41 – UAR 2014 - PLBS for their help and advice with the flow cytometry experiments. The mass spectrometry and tumoroid experiments were carried out at the OrganOmics core facility of PRISM Inserm U1192, which is accredited by GIS IBiSA and members of the national proteomic infrastructure INBS ProFI. The authors wish to acknowledge OrganOmics for the technical and human resources support.

AUTHOR CONTRIBUTIONS

A.R.-R. and M.D. wrote the manuscript with support from all of the authors. M.D. and M.S. conceived the project. M.D., M.S., and I.F. have obtained fundings. A.R.-R. and L.Z.C. performed the experiments and collected and analyzed the data. A.R.-R. and M.D. were involved in the experimental design. N.H. conducted the clinical study and provided the tumor samples. S.S.-D. performed the light-sheet microscopy acquisition and image analysis. All authors contributed to the article and approved the submitted version.

DECLARATION OF INTERESTS

The authors declare no competing interests.

Received: January 3, 2024
Revised: April 26, 2024
Accepted: May 17, 2024
Published: June 10, 2024

REFERENCES

1. Langhans, S.A. (2018). Three-Dimensional in Vitro Cell Culture Models in Drug Discovery and Drug Repositioning. Front. Pharmacol. *9*, 6. https://doi.org/10.3389/FPHAR.2018.00006.
2. Broutier, L., Mastrogiovanni, G., Verstegen, M.M., Francies, H.E., Gavarró, L.M., Bradshaw, C.R., Allen, G.E., Arnes-Benito, R., Sidorova, O., Gaspersz, M.P., et al. (2017). Human primary liver cancer-derived organoid cultures for disease modeling and drug screening. Nat. Med. *23*, 1424–1435. https://doi.org/10.1038/nm.4438.
3. Sachs, N., de Ligt, J., Kopper, O., Gogola, E., Bounova, G., Weeber, F., Balgobind, A.V., Wind, K., Gracanin, A., Begthel, H., et al. (2018). A Living Biobank of Breast Cancer Organoids Captures Disease Heterogeneity. Cell *172*, 373–386.e10. https://doi.org/10.1016/j.cell.2017.11.010.
4. Nuciforo, S., Fofana, I., Matter, M.S., Blumer, T., Calabrese, D., Boldanova, T., Piscuoglio, S., Wieland, S., Ringnalda, F., Schwank, G., et al. (2018). Organoid Models of Human Liver Cancers Derived from Tumor Needle Biopsies. Cell Rep. *24*, 1363–1376. https://doi.org/10.1016/j.celrep.2018.07.001.
5. Lee, S.H., Hu, W., Matulay, J.T., Silva, M.V., Owczarek, T.B., Kim, K., Chua, C.W., Barlow, L.J., Kandoth, C., Williams, A.B., et al. (2018). Tumor Evolution and Drug Response in Patient-Derived Organoid Models of Bladder Cancer. Cell *173*, 515–528.e17. https://doi.org/10.1016/j.cell.2018.03.017.
6. Law, A.M.K., Rodriguez de la Fuente, L., Grundy, T.J., Fang, G., Valdes-Mora, F., and Gallego-Ortega, D. (2021). Advancements in 3D Cell Culture Systems for Personalizing Anti-Cancer Therapies. Front. Oncol. *11*, 782766. https://doi.org/10.3389/FONC.2021.782766.
7. Raffo-Romero, A., Aboulouard, S., Bouchaert, E., Rybicka, A., Tierny, D., Hajjaji, N., Fournier, I., Salzet, M., and Duhamel, M. (2023). Establishment and characterization of canine mammary tumoroids for translational research. BMC Biol. *21*, 23. https://doi.org/10.1186/S12915-023-01516-2/FIGURES/8.
8. Sato, T., Vries, R.G., Snippert, H.J., Van De Wetering, M., Barker, N., Stange, D.E., Van Es, J.H., Abo, A., Kujala, P., Peters, P.J., and Clevers, H. (2009). Single Lgr5 stem cells build crypt-villus structures in vitro without a mesenchymal niche. Nat *459*, 262–265, 2009 4597244. https://doi.org/10.1038/nature07935.
9. Neal, J.T., Li, X., Zhu, J., Giangarra, V., Grzeskowiak, C.L., Ju, J., Liu, I.H., Chiou, S.H., Salahudeen, A.A., Smith, A.R., et al. (2018). Organoid Modeling of the Tumor Immune Microenvironment. Cell *175*, 1972–1988.e16. https://doi.org/10.1016/j.cell.2018.11.021.
10. Öhlund, D., Handly-Santana, A., Biffi, G., Elyada, E., Almeida, A.S., Ponz-Sarvise, M., Corbo, V., Oni, T.E., Hearn, S.A., Lee, E.J., et al. (2017). Distinct populations of inflammatory fibroblasts and myofibroblasts in pancreatic cancer. J. Exp. Med. *214*, 579–596. https://doi.org/10.1084/JEM.20162024.
11. Chakrabarti, J., Holokai, L., Syu, L., Steele, N.G., Chang, J., Wang, J., Ahmed, S., Dlugosz, A., and Zavros, Y. (2018). Hedgehog signaling induces PD-L1 expression and tumor cell proliferation in gastric cancer. Oncotarget *9*, 37439–37457. https://doi.org/10.18632/ONCOTARGET.26473.
12. Schnalzger, T.E., Groot, M.H., Zhang, C., Mosa, M.H., Michels, B.E., Röder, J., Darvishi, T., Wels, W.S., and Farin, H.F. (2019). 3D model for CAR-mediated cytotoxicity using patient-derived colorectal cancer organoids. EMBO J. *38*. https://doi.org/10.15252/EMBJ.2018100928.
13. Gentles, A.J., Newman, A.M., Liu, C.L., Bratman, S.V., Feng, W., Kim, D., Nair, V.S., Xu, Y., Khuong, A., Hoang, C.D., et al. (2015). The prognostic landscape of genes and infiltrating immune cells across human cancers. Nat. Med. *21*, 938–945. https://doi.org/10.1038/NM.3909.
14. Song, M., Yeku, O.O., Rafiq, S., Purdon, T., Dong, X., Zhu, L., Zhang, T., Wang, H., Yu, Z., Mai, J., et al. (2020). Tumor derived UBR5 promotes ovarian cancer growth and metastasis through inducing immunosuppressive macrophages. Nat. Commun. *11*, 6298–6316. https://doi.org/10.1038/s41467-020-20140-0.
15. Orrantia-Borundam, E., Anchondo-Nuñez, P., Acuña-Aguilar, L.E., Gómez-Valles, F.O., and Ramírez Valdespino, C.A. (2022). Subtypes of Breast Cancer. In Breast Cancer, H.N. Mayrovitz, ed. https://doi.org/10.36255/exon-publications-breast-cancer-subtypes.
16. Dekkers, J.F., van Vliet, E.J., Sachs, N., Rosenbluth, J.M., Kopper, O., Rebel, H.G., Wehrens, E.J., Piani, C., Visvader, J.E., Verissimo, C.S., et al. (2021). Long-term culture, genetic manipulation and xenotransplantation of human normal and breast cancer organoids. Nat. Protoc. *16*, 1936–1965. https://doi.org/10.1038/S41596-020-00474-1.
17. Hasan, M.N., Capuk, O., Patel, S.M., and Sun, D. (2022). The Role of Metabolic Plasticity of Tumor-Associated Macrophages in Shaping the Tumor Microenvironment Immunity. Cancers *14*, 3331. https://doi.org/10.3390/cancers14143331.
18. Hanahan, D. (2022). Hallmarks of Cancer: New Dimensions. Cancer Discov. *12*, 31–46. https://doi.org/10.1158/2159-8290.CD-21-1059.

19. Zhong, W., Lu, Y., Han, X., Yang, J., Qin, Z., Zhang, W., Yu, Z., Wu, B., Liu, S., Xu, W., et al. (2023). Upregulation of exosome secretion from tumor-associated macrophages plays a key role in the suppression of anti-tumor immunity. Cell Rep. *42*, 113224. https://doi.org/10.1016/j.celrep.2023.113224.

20. Evans, R., Flores-Borja, F., Nassiri, S., Miranda, E., Lawler, K., Grigoriadis, A., Monypenny, J., Gillet, C., Owen, J., Gordon, P., et al. (2019). Integrin-Mediated Macrophage Adhesion Promotes Lymphovascular Dissemination in Breast Cancer. Cell Rep. *27*, 1967–1978.e4. https://doi.org/10.1016/j.celrep.2019.04.076.

21. Chen, X., Yang, M., Yin, J., Li, P., Zeng, S., Zheng, G., He, Z., Liu, H., Wang, Q., Zhang, F., and Chen, D. (2022). Tumor-associated macrophages promote epithelial-mesenchymal transition and the cancer stem cell properties in triple-negative breast cancer through CCL2/AKT/β-catenin signaling. Cell Commun. Signal. *20*, 92. https://doi.org/10.1186/s12964-022-00888-2.

22. Wang, Y.C., Wang, X., Yu, J., Ma, F., Li, Z., Zhou, Y., Zeng, S., Ma, X., Li, Y.R., Neal, A., et al. (2021). Targeting monoamine oxidase A-regulated tumor-associated macrophage polarization for cancer immunotherapy. Nat. Commun. *12*, 3530–3617. https://doi.org/10.1038/s41467-021-23164-2.

23. Cassetta, L., Fragkogianni, S., Sims, A.H., Swierczak, A., Forrester, L.M., Zhang, H., Soong, D.Y.H., Cotechini, T., Anur, P., Lin, E.Y., et al. (2019). Human Tumor-Associated Macrophage and Monocyte Transcriptional Landscapes Reveal Cancer-Specific Reprogramming, Biomarkers, and Therapeutic Targets. Cancer Cell *35*, 588–602.e10. https://doi.org/10.1016/j.ccell.2019.02.009.

24. Deligne, C., and Midwood, K.S. (2021). Macrophages and Extracellular Matrix in Breast Cancer: Partners in Crime or Protective Allies? Front. Oncol. *11*, 620773. https://doi.org/10.3389/FONC.2021.620773.

25. Olson, O.C., Kim, H., Quail, D.F., Foley, E.A., Joyce, J.A., and Joyce, J.A. (2017). Tumor-Associated Macrophages Suppress the Cytotoxic Activity of Antimitotic Agents. Cell Rep. *19*, 101–113. https://doi.org/10.1016/j.celrep.2017.03.038.

26. Guillen, K.P., Fujita, M., Butterfield, A.J., Scherer, S.D., Bailey, M.H., Chu, Z., DeRose, Y.S., Zhao, L., Cortes-Sanchez, E., Yang, C.H., et al. (2022). A human breast cancer-derived xenograft and organoid platform for drug discovery and precision oncology. Nat. Cancer *3*, 232–250. https://doi.org/10.1038/s43018-022-00337-6.

27. Cattaneo, C.M., Dijkstra, K.K., Fanchi, L.F., Kelderman, S., Kaing, S., van Rooij, N., van den Brink, S., Schumacher, T.N., and Voest, E.E. (2019). Tumor organoid–T-cell coculture systems. Nat. Protoc. *15*, 15–39. https://doi.org/10.1038/s41596-019-0232-9.

28. Dijkstra, K.K., Cattaneo, C.M., Weeber, F., Chalabi, M., van de Haar, J., Fanchi, L.F., Slagter, M., van der Velden, D.L., Kaing, S., Kelderman, S., et al. (2018). Generation of Tumor-Reactive T Cells by Co-culture of Peripheral Blood Lymphocytes and Tumor Organoids. Cell *174*, 1586–1598.e12. https://doi.org/10.1016/j.cell.2018.07.009.

29. Meng, Q., Xie, S., Gray, G.K., Dezfulian, M.H., Li, W., Huang, L., Akshinthala, D., Ferrer, E., Conahan, C., Perea Del Pino, S., et al. (2021). Original research: Empirical identification and validation of tumor-targeting T cell receptors from circulation using autologous pancreatic tumor organoids. J. Immunother. Cancer *9*, 3213. https://doi.org/10.1136/JITC-2021-003213.

30. Kong, J.C.H., Guerra, G.R., Millen, R.M., Roth, S., Xu, H., Neeson, P.J., Darcy, P.K., Kershaw, M.H., Sampurno, S., Malaterre, J., et al. (2018). Tumor-Infiltrating Lymphocyte Function Predicts Response to Neoadjuvant Chemoradiotherapy in Locally Advanced Rectal Cancer. JCO Precis. Oncol. *2*, 1–15. https://doi.org/10.1200/PO.18.00075.

31. Zhou, G., Lieshout, R., van Tienderen, G.S., de Ruiter, V., van Royen, M.E., Boor, P.P.C., Magré, L., Desai, J., Köten, K., Kan, Y.Y., et al. (2022). Modelling immune cytotoxicity for cholangiocarcinoma with tumour-derived organoids and effector T cells. Br. J. Cancer, 649–660. https://doi.org/10.1038/s41416-022-01839-x.

32. de Araujo Junior, R.F., Eich, C., Jorquera, C., Schomann, T., Baldazzi, F., Chan, A.B., and Cruz, L.J. (2020). Ceramide and palmitic acid inhibit macrophage-mediated epithelial-mesenchymal transition in colorectal cancer. Mol. Cell. Biochem. *468*, 153–168. https://doi.org/10.1007/S11010-020-03719-5.

33. Masquelier, J., Alhouayek, M., Terrasi, R., Bottemanne, P., Paquot, A., and Muccioli, G.G. (2018). Lysophosphatidylinositols in inflammation and macrophage activation: Altered levels and anti-inflammatory effects. Biochim. Biophys. acta. Mol. cell Biol. lipids *1863*, 1458. https://doi.org/10.1016/J.BBALIP.2018.09.003.

34. Vasseur, S., and Guillaumond, F. (2022). Lipids in cancer: a global view of the contribution of lipid pathways to metastatic formation and treatment resistance. Oncog., 46. https://doi.org/10.1038/s41389-022-00420-8.

35. Lewis, A.C., Wallington-Beddoe, C.T., Powell, J.A., and Pitson, S.M. (2018). Targeting sphingolipid metabolism as an approach for combination therapies in haematological malignancies. Cell Death Discov. *4*, 72. https://doi.org/10.1038/s41420-018-0075-0.

36. Ruffell, B., and Coussens, L.M. (2015). Macrophages and Therapeutic Resistance in Cancer. Cancer Cell *27*, 462–472. https://doi.org/10.1016/J.CCELL.2015.02.015.

37. Duhamel, M., Rose, M., Rodet, F., Murgoci, A.N., Zografidou, L., Régnier-Vigouroux, A., Vanden Abeele, F., Kobeissy, F., Nataf, S., Pays, L., et al. (2018). Paclitaxel Treatment and Proprotein Convertase 1/3 (PC1/3) Knockdown in Macrophages is a Promising Antiglioma Strategy as Revealed by Proteomics and Cytotoxicity Studies. Mol. Cell. Proteomics *17*, 1126–1143. https://doi.org/10.1074/mcp.RA117.000443.

38. Wiśniewski, J.R., Zougman, A., Nagaraj, N., and Mann, M. (2009). Universal sample preparation method for proteome analysis. Nat. Methods *6*, 359–362. https://doi.org/10.1038/nmeth.1322.

39. Klein, O., Strohschein, K., Nebrich, G., Oetjen, J., Trede, D., Thiele, H., Alexandrov, T., Giavalisco, P., Duda, G.N., von Roth, P., et al. (2014). MALDI imaging mass spectrometry: Discrimination of pathophysiological regions in traumatized skeletal muscle by characteristic peptide signatures. Proteomics *14*, 2249–2260. https://doi.org/10.1002/PMIC.201400088.

40. Trede, D., Kobarg, J.H., Oetjen, J., Thiele, H., Maass, P., and Alexandrov, T. (2012). On the importance of mathematical methods for analysis of MALDI-imaging mass spectrometry data. J. Integr. Bioinform. *9*, 189. https://doi.org/10.2390/BIECOLL-JIB-2012-189.

41. Alexandrov, T., Becker, M., Deininger, S.O., Ernst, G., Wehder, L., Grasmair, M., Von Eggeling, F., Thiele, H., and Maass, P. (2010). Spatial segmentation of imaging mass spectrometry data with edge-preserving image denoising and clustering. J. Proteome Res. *9*, 6535–6546. https://doi.org/10.1021/PR100734Z/SUPPL_FILE/PR100734Z_SI_001.PDF.

42. Tyanova, S., and Cox, J. (2018). Perseus: A Bioinformatics Platform for Integrative Analysis of Proteomics Data in Cancer Research. Methods Mol. Biol. *1711*, 133–148. https://doi.org/10.1007/978-1-4939-7493-1_7.

43. Tyanova, S., Temu, T., Sinitcyn, P., Carlson, A., Hein, M.Y., Geiger, T., Mann, M., and Cox, J. (2016). The Perseus computational platform for comprehensive analysis of (prote)omics data. Nat. Methods *13*, 731–740. https://doi.org/10.1038/nmeth.3901.

44. Pathan, M., Keerthikumar, S., Ang, C.S., Gangoda, L., Quek, C.Y.J., Williamson, N.A., Mouradov, D., Sieber, O.M., Simpson, R.J., Salim, A., et al. (2015). FunRich: An open access standalone functional enrichment and interaction network analysis tool. Proteomics *15*, 2597–2601. https://doi.org/10.1002/PMIC.201400515.

STAR★METHODS

KEY RESOURCES TABLE

REAGENT or RESOURCE	SOURCE	IDENTIFIER
Antibodies		
BV786 Mouse anti-human CD86 (Clone BU63)	BD biosciences	Cat# 747526;RRID: AB_2744102
BF786 Mouse IgG1, κ Isotype Control (Clone X40)	BD biosciences	Cat# 563330;RRID: AB_2869484
BV421 Mouse anti-human CD163 (Clone GHI/61)	BD biosciences	Cat# 562643;RRID: AB_2737697
BV421 Mouse IgG1, κ Isotype Control (Clone X40)	BD biosciences	Cat# 562438.RRID: AB_11207319
BV605 Mouse anti-human CD11B (Clone ICRF44)	BD biosciences	Cat# 562721;RRID: AB_2737745
BV605 Mouse IgG1, κ Isotype Control (Clone X40)	BD biosciences	Cat# 562652;RRID: AB_2714005
Donkey anti-Mouse IgG (H + L), Alexa Fluor™ 488 (1/200)	Fisher scientific	Cat# A21202;RRID: AB_141607
Monoclonal Mouse anti-human CD68 (1/50)	Santa Cruz Biotechnology	Cat# sc-17832;RRID: AB_627157
PE Mouse anti-human CD206 (Clone 19.2)	BD biosciences	Cat# 555954;RRID: AB_396250
PE Mouse IgG1, κ Isotype Control (Clone MOPC-21)	BD biosciences	Cat# 555749;RRID: AB_396091
PE-Cy™5 Mouse anti-human CD80 (Clone L307.4)	BD biosciences	Cat# 559370;RRID: AB_397239
PE-Cy™5 Mouse IgG1, κ Isotype Control (Clone MOPC-21)	BD biosciences	Cat# 555750;RRID: AB_396092
PE-Cy™7 Mouse anti-human HLA-DR (Clone G46-6)	BD biosciences	Cat# 560651;RRID: AB_1727528
PE-Cy™7 Mouse IgG2a, κ Isotype Control (Clone G155-178)	BD biosciences	Cat# 557907;RRID: AB_647254
Biological samples		
Blood from donor	French Blood Establishment	N/A
Breast cancer biopsies tissue	Oscar Lambret Cancer center and a French Ethical Committee	Study IdRCB 2021-A00670-41
Chemicals, peptides, and recombinant proteins		
A83-01	Tocris	Cat# 2939
Advanced DMEM/F12	Invitrogen	Cat# 12634-034
Ammonium bicarbonate, BioUltra ≥99.5%	Sigma-aldrich	Cat# 09830
Ammonium persulfate, BioUltra, for molecular biology, ≥98.0%	Sigma-aldrich	Cat# 09913
B27 supplement	Gibco	Cat# 17504-44
Beta-Estradiol, suitable for cell culture	Sigma	Cat# E2758-250MG
Bovine Serum Albumin	Merck	Cat# A3059
Collagenase from Clostridium histolyticum	Sigma	Cat# C5138-100MG
CytoTell™ Green	AAT Bioquest	Cat# 22253
Dimethyl sulfoxide (DMSO)	Sigma-Aldrich	Cat# D5879
DL-Dithiothreitol (DTT)	VWR Life Science	Cat# 97063-760
DPBS, no calcium, no magnesium	Fisher Scientific	Cat# 14190-094

(*Continued on next page*)

Continued

REAGENT or RESOURCE	SOURCE	IDENTIFIER
EGF	Peprotech	Cat# AF-100-15
Enzyme (1X) TrypLE™ Express, rouge de phénol	Gibco	Cat# 12605010
Fetal Bovine Serum, qualified, heat inactivated, E.U.-approved, South America Origin	Gibco	Cat# 10500064
FGF 10	Peprotech	Cat# 100-26
FGF 7	Peprotech	Cat# 100-19
Ficoll®-Paque Premium	Merck	Cat# GE17-5442-02
Forskolin, from Coleus forskohlii	Sigma	Cat# F6886-10MG
GlutaMax 100x	Invitrogen	Cat# 12634-034
HEPES	Invitrogen	Cat# 15630-056
Hoechst 33342	Eurogentec	Cat# AS-83218
Hyaluronidase from Streptomyces hyalurolyticus	Sigma	Cat# H1136-1AMP
Hydrocortisone, suitable for cell culture	Sigma	Cat# H0888-1G
Invitrogen™ Tampon de lyse RBC (multi-espèces) eBioscience™ 10X	Fisher Scientific	Cat# 15270658
Iodoacetamide (IAA)	Sigma-Aldrich	Cat# I1149
Macrophage Detachment Solution DXF	PromoCell Inc	Cat# C-41330
Matrigel™ matrix for organoid culture	Corning	Cat# 356255
N-Acetylcysteine	Sigma	Cat# A9165-5g
Neuregulin 1	Peprotech	Cat# 100-03
Nicotinamide	Sigma	Cat# N0636
Noggin	Peprotech	Cat# 120-10C
Penicillin/Streptomycin	Invitrogen	Cat# 15140-122
Penicillin-Streptomycin (10,000 U/mL)	Gibco	Cat# 15140122
Primocin	Invivogen	Cat# Ant-pm-1
Recombinant Human M-CSF	Ozyme	Cat# BLE574802
SB202190	Sigma	Cat# S7067
Sodium chloride	Fisher Chemical	Cat# S/3161/60
Trypsin/Lys-C Mix, Mass Spec Grade	Promega	Cat# V5073
Trypsin-EDTA (0.05%), phenol red	Gibco	Cat# 5300054
Urea Ultra-Pure	Euromedex	Cat# EU0014B
Water, UHPLC-MS	Fisher Scientific	Cat# 15339865
X-VIVOTM 15 Serum-free Hematopoietic Cell Medium	Lonza	Cat# 02-053Q
Y-27632	Abmole	Cat# M1817
Critical commercial assays		
CellTiter-Glo® 3D Cell Viability Assay	Promega	Cat# G9681
LIVE/DEAD™ Fixable Near-IR Dead Cell Staining Kit for excitation at 633 or 635 nm	Invitrogen™	Cat# L34975
Deposited data		
Mass spectrometry proteomics data	This paper	ProteomeXchange Consortium via the PRIDE partner repository; dataset identifier: PXD052016
Software and algorithms		
Adobe Illustrator	Adobe	RRID:SCR_010279
Biorender	Biorender.com	RRID:SCR_018361
Dia-NN	Version 1.8.1-Open source	https://github.com/vdemichev/DiaNN
Graphpad Prism v6	www.graphpad.com	www.graphpad.com/scientific-software/prism/
ImageJ version 1.54f	Open Source	https://imagej.net/ij/

(*Continued on next page*)

Continued

REAGENT or RESOURCE	SOURCE	IDENTIFIER
IMARIS version 10.0	Bitplane Inc., 2019	https://imaris.oxinst.com/
Kaluza	Beckman Coulter	N/A
Perseus 1.6.15.0	Tyanova et al., 2016[39,40]	https://doi.org/10.1038/nmeth.39
Scils Lab software	Version 2022a Pro	https://store.bruker.com/products/scils-lab-core
Other		
Amicon Ultra-0.5 Centrifugal Filter Unit 30 kDa	Merck	Cat# UFC503024
EVOTIP PURE, 1 × 96 TIPS	Evosep	Cat# EV2011

RESOURCE AVAILABILITY

Lead contact

Further information and requests for resources, reagents or biological materials should be directed to and will be fulfilled by the lead contact: Marie Duhamel (marie.duhamel@univ-lille.fr).

Materials availability

- No new or unique reagents were generated in this study.
- Matrigel basement membrane is a limited resource due to high demand and backorders. To avoid potential protein variation in Matrigel, we use a commercial Matrigel designed for organoids, aimed at minimizing variation. The details are given in the Key Resource Table.

Data and code availability

- The mass spectrometry proteomics data have been deposited with the ProteomeXchange Consortium via the PRIDE partner repository with the dataset identifier PXD052016.
- This study does not report original code.
- Any additional information required to reanalyze the data reported in this work paper is available from the lead contact upon request.

EXPERIMENTAL MODEL AND STUDY PARTICIPANT DETAILS

Human patients' tissue collection

This study was conducted on human breast tumor tissue, luminal subtypes. All human breast tumor tissues were obtained from different patients undergoing surgery for early breast cancer. Fresh tumor tissue was provided by the pathologist for organoid culture. The sample was anonymized before transfer to the laboratory. The study was approved by the local research committee of the Oscar Lambret cancer center and a French Ethical Committee (study IdRCB 2021-A00670-41). Written informed consent for the study was obtained from the patient before each procedure.

Purification of blood PBMCs

Peripheral blood mononuclear cells (PBMCs) were isolated by Ficoll density gradient centrifugation protocol (Cytiva, France) from venous blood samples (EDTA tubes) obtained from healthy donors. Blood was obtained from the French Blood Establishment (EFS, Lille, France). All blood samples were processed within 24 h of collection.

METHOD DETAILS

Tissue processing

Fresh biopsies of approximately 10 mm in length and 2 mm in diameter were transported from the Oscar Lambret Cancer Center to the laboratory on the day of sampling. The sample was used fresh for tumoroid culture, for which the tumor fragment was minced into 1 mm^3 pieces prior to enzymatic digestion as described below.

Tumoroid culture

The tumor tissue biopsy was minced and placed in digestion medium in a reduced volume of 2 mL to avoid loss of material. The digestion medium consisted of Hank's balanced salt solution (HBSS, Gibco) with antibiotics and antifungals (1X penicillin/streptomycin, 1X amphoteromicin) containing 1 mg/mL collagenase type IV (Sigma) and 5 U/mL hyaluronidase (Sigma). The tumor tissue was digested at 37°C for 2 h and mixed every 15 min to facilitate digestion. After digestion, 6 mL of HBSS with antibiotics was added

and the cell suspension was filtered through a 100 μm filter (Dutcher) to retain residual tissue pieces. The suspension was centrifuged at 300 g for 5 min. If red pellet was visible, the erythrocytes were lysed in 1 mL red blood cell lysis buffer (RBC, Invitrogen) for 5 min at room temperature. The suspension was then completed with 6 mL HBSS with antibiotics and centrifuged at 300 g for 5 min. The cell pellet was resuspended in Matrigel a reduced growth factor solubilized basement membrane matrix optimized for organoid culture (Matrigel, Corning 356255) and plated dropwise into 24-well plates. Due to the limited amount of cells in the biopsy, only one to two drops were prepared per biopsy. Matrigel was allowed to solidify in the incubator for 30 min and then 500 μL of complete culture medium was added. The complete tumoroid culture expansion medium Type 1 consisted of Advanced DMEM (Gibco) supplemented with 1X Glutamax, 10 mM HEPES, 1X penicillin/streptomycin, 1X amphoteromicin, 50 μg/mL Primocin, 1X B27 supplement, 5 mM nicotinamide, 1.25 mM N-acetylcysteine, 250 ng/mL R-spondin 1, 5 nM heregulinβ-1, 100 ng/mL noggin, 20 ng/mL FGF-10, 5 ng/mL FGF-7, 5 ng/mL EGF, 500 nM A83-01, 500 nM SB202190 and 5 μM Y-27632. Type 2 has the same composition with the addition of the following components: hydrocortiosone 0.5 μg/mL, β-estradiol 100 nM and forskolin 10 μM.

When the tumoroids were confluent, occupying approximately 70–80% of the Matrigel drop, they were divided for multiplication. Cold PBS was used to harvest the tumoroids from the Matrigel, slowly mixing back and forth until the Matrigel was liquefied. They were collected in a 15 mL Falcon pre-coated with PBS containing 1% BSA solution to prevent the tumoroids from adhering to the tube. The tumoroids were centrifuged at 300 g for 5 min at 4°C and then digested with TrypLE solution (Gibco) for 5 min at 37°C. After enzymatic neutralization and washing with HBSS medium, the tumoroid fragments were resuspended in Matrigel and reseeded as described above to allow the formation of new tumoroids.

Isolation of PBMCs from blood

PBMCs were obtained from blood using the Ficoll gradient technique. First, the blood was diluted by half in a solution of PBS with 0.1% EDTA. Then 10 mL of the diluted blood was gently layered over 7 mL of Ficoll in 50 mL tubes, which were then centrifuged at 2200 rpm for 25 min at 20°C with the brake off. The resulting PBMC fractions from each tube were combined in a new tube containing 10 mL of PBS with 0.1% EDTA, followed by centrifugation at 1300 rpm for 10 min at 20°C. After discarding the supernatant, the pellet was washed with 10 mL PBS containing 0.1% EDTA and centrifuged at 1200 rpm for 10 min at 20°C. This washing process was repeated at 900 rpm for 10 min at 20°C and when the pellet appeared red, the erythrocytes were lysed using RBC lysis buffer (Invitrogen, France) diluted 1X in water for 5 min at room temperature. The RBC lysis buffer was then diluted with 10 mL of EDTA-free PBS and the tubes centrifuged again at 900 rpm for 10 min at 20°C. The resulting cell pellet was resuspended in 10 mL of serum-free RPMI-1641 medium (containing RPMI-1641, 1X Glutamax, and 1X penicillin/streptomycin) and counted to either isolate the monocytes immediately or to freeze the PBMCs for future use.

For monocyte isolation, 10 million PBMCs were cultured in 10 cm^3 plates for 2 h at 37°C. Once adherent, the monocytes were washed twice with PBS. Then 10 mL of complete medium RPMI-1641 with M-CSF (RPMI-1641, 10% fetal bovine serum, 1X Glutamax, 1X penicillin/streptomycin, and 50 ng/mL MCS-F) was added to stimulate their differentiation into macrophages for 7 days. For freezing, 3 million PBMCs were placed in freezing medium (90% serum +10% DMSO) and stored at −80°C. For longer storage, they were transferred to liquid nitrogen.

PBMC thawing

Two different wash media (RPMI, 1% serum, 0.1% EDTA or PBS, 0.1% EDTA) were tested for PBMC thawing. To thaw the PBMCs, we prepared a 5 mL vial of warm wash medium, and once the cryotube was thawed in the 37°C water bath, we added 1 mL of warm wash medium directly to the cryotube and placed the 2 mL into the prepared 5 mL vial. We then washed the cryotube with 1 mL of warm medium and collected the whole in the Falcon tube. The Falcon was centrifuged at 500xg for 10 min. The supernatant was removed and resuspended with 6 mL of warm washing medium and centrifuged again at 500xg for 10 min. The supernatant was removed. The cell pellet was resuspended with an optimized macrophage differentiation medium based on X-VIVOTM 15 serum-free haematopoietic cell medium (X-VIVOTM 15, 10% serum, 10 mM HEPES, 1 mM sodium pyruvate, 1% penicillin/streptomycin, 1% L-glutamine, 50 ng/mL M-CSF) and incubated at 37°C for 7 days. Half of the medium was gently replaced with the same fresh medium 48 h later. PBMC were incubated at 37°C for 7 days to induce isolation and differentiation into macrophages for 7 days.

Macrophage recovery

For the trypsin detachment protocol, the plates were washed 3 times with 10 mL of PBS each time. Then, 1 mL of trypsin per plate was added and incubated at 37°C for 10 min, then the trypsin was mixed by rocking the trypsin in the plate and the plate was tapped to promote detachment and returned to 37°C for a further 10 min. The trypsin was then mixed again, removed from the plate and collected in a Falcon with 15 mL of complete culture medium (RPMI-1641, 10% serum, 1X Glutamax, 1X penicillin/streptomycin). The plates were then washed with 5 mL PBS, immediately collected in the same recovery Falcon and the plates were observed, normally there should be no adherent cells left. If some cells were still attached, 1 mL of a mixture of 50% trypsin and 50% Macrophage Detachment Solution (PromoCell, France) was used and incubated at 37°C for a further 10 min. The mixture containing the remaining cells was then removed from the plate, collected in the previous Falcon and the plate was washed with 5 mL PBS. The Falcon was centrifuged at 500xg for 10 min. The supernatant was removed, the cells resuspended in complete culture medium (RPMI-1641, 10% serum, 1X Glutamax, 1X penicillin/streptomycin) and counted.

For the Macrophage Detachment Solution (PromoCell, France) detachment protocol, the plates were washed 3 times with 10 mL of PBS each time. The macrophages were then detached by adding 8 mL of Macrophage Detachment Solution and incubated at 2°C–8°C for 30 min, followed by 1 h at room temperature. The harvested macrophages were placed in a coated tube containing equal volumes of PBS, 0.1% EDTA, 0.1% BSA. They were then centrifuged at 400xg for 15 min at room temperature. The supernatant was removed. The cells were then washed with PBS, 0.1% EDTA, 0.1% BSA. The cells were centrifuged again for 15 min at 400xg at room temperature. The supernatant was removed and the cells were resuspended in PBS, 0.1% EDTA and counted.

Tumoroid and macrophage co-culture models

We have used 3 different co-culture methods: one semi-liquid and two solid conditions in Matrigel. In all protocols, the first step involved the recovery of tumoroids and macrophages prior to co-culture. Tumoroids were recovered through two trypsinisations using TrypLE solution (Gibco), as previously described. Similarly, macrophages were harvested according to the aforementioned method, with or without Cytotell staining for macrophage tracking. Subsequently, both cell types were counted, and we maintained a macrophage concentration of 30% relative to the tumoroid cells.

In the semi-liquid co-culture method, non-adherent PrimeSurface plates (MS-9024OZ) were used, where macrophages were mixed with tumoroids in complete tumoroid culture medium supplemented with 2% Matrigel. We ensured thorough mixing of Matrigel with the cold culture medium to prevent immediate solidification before incorporation.

For the two solid co-culture methods, a 1 μM Transwell was used, with a drop of Matrigel positioned directly in the center of the filter. Two distinct techniques were implemented: (i) placing tumoroids in the Matrigel followed by addition of 200 μL of complete culture medium containing macrophages after 30 min at 37°C, or (ii) directly mixing macrophages and tumoroids in the Matrigel, followed by addition of 200 μL of complete tumoroid culture medium after 30 min. The Transwell remainined in the incubator at 37°C for 1 h, after which 600 μL of culture medium was added to the bottom compartment.

Consistency was ensured within each replicate by employing cells sourced from the same patient tumor, while macrophages were derived from the same batch to minimize variability.

Cytotell cell labeling

To dynamically track the macrophages in the models, we labeled the PBMC with CytoTell UltraGreen (22240, AAT Bioquest). We mixed 500 μL PBS containing 500000 macrophages with 1 μL CytoTell UltraGreen. The tubes were incubated for 30 min at 37°C. We then centrifuged them to remove the supernatant before adding them to the co-culture with the tumoroids. We followed the development of the co-culture over time by microscopy before fixing the co-culture for immunofluorescence analysis.

Immunofluorescence of macrophages

After the fresh or frozen macrophages were detached, they were counted and 50000 macrophages were cultured on coverslips in a 4-well plate for 2 days. The coverslips were then placed in a humidified box to prevent dessication. The coverslips were fixed with 4% paraformaldehyde for 20 min at room temperature. After fixation, the coverslips were rinsed twice in PBS and pre-incubated in blocking buffer (consisting of 0.3% Triton, 5% normal donkey serum (NDS) and 2% BSA) for 1 h at room temperature. The samples were then incubated overnight at 4°C with the anti-CD68 primary antibody diluted in the above blocking buffer (1:50, Santa Cruz). After a further set of three washes with PBS, the coverslips were incubated for 1 h at room temperature with donkey anti-mouse secondary antibody, conjugated to Alexa Fluor 488 (1:200, Invitrogen, Carlsbad CA, USA) in blocking buffer. Coverslips were then rinsed with PBS, and nuclei counterstained with Hoechst 33342 fluorescent dye (at 1:10,000, Invitrogen, Carlsbad CA, USA) for 20 min at 4°C. Finally, coverslips were mounted onto microscope slides using Dako Fluorescent Mounting Medium (Agilent, Santa Clara CA, USA). Samples without the addition of the primary antibody were used as negative controls. Slides were imaging using a Zeiss LSM700 confocal microscope attached to a Zeiss Axiovert 200 M with an EC Plan-Neofluar 40×/1.30 numerical aperture and an oil immersion objective (Carl Zeiss AG, Oberkochen, Germany). Zen software was employed for image processing, applied uniformly to both the entire images and control samples. Images shown are independent triplicates.

Immunofluorescence of macrophages in the 3D co-culture tumoroid models

Immunohistochemical staining was performed on the three co-culture models. For the semi-liquid co-culture model, tumoroids were harvested and placed in a 4-well Lab-Tek coverglass (155383) that had previously been coated with poly-D-lysine for 15 min. The tumoroids were incubated for 24 h at 37°C to allow the tumoroids to adhere to the bottom of the Lab-Tek coverglass. For the solid models, they were gently washed with PBS, removed from the Transwell with a spatula and placed in a Lab-Tek coverglass. The immunofluorescence protocol was then performed directly in the Lab-Tek coverglass until observation. At each stage, care was taken to avoid loss of material when removing the liquid.

First, the models were fixed with 600 μL of fixation buffer (2% paraformaldehyde in PBS with 0.1% glutaraldehyde) and incubated at 4°C for 24 h. The fixed tumoroids were then washed with PBS and treated with a permeabilization buffer (1% Triton X-100, 0.1% Tween, in PBS with 0.1 M glycine) over a weekend at 4°C to allow the antibodies to enter the cells. The models were rinsed twice with IF buffer (0.4% Triton X-100, 0.1% Tween, in PBS with 0.1 M glycine) and then incubated overnight at 4°C with blocking buffer (0.4% Triton X-100, 0.1% Tween, 10% normal donkey serum (NDS), 2% BSA, in PBS with 0.1 M glycine) to block non-specific binding sites. Tumoroids were incubated overnight at 4°C with primary antibody anti-CD68 (Santa Cruz - E−11) diluted 1/50 in blocking buffer.

Subsequent steps were performed in the dark. After several washes with IF buffer to remove unbound primary antibody, the tumoroids were incubated with donkey anti-mouse secondary antibody conjugated to Alexa Fluor 488 (1:200, Invitrogen, Carlsbad CA, USA) in blocking buffer overnight at 4°C in the dark. The tumoroids were then rinsed with PBS and the nuclei counterstained with Hoechst 33,342 fluorescent dye (1/500, Invitrogen, Carlsbad CA, USA) overnight at 4°C. Finally, the tumoroids were subjected to a transparency protocol using formamide and PEG (polyethylene glycol) to improve 3D observation. The tumoroids were incubated in a mixture of 25% formamide and 10% PEG for 1 h, followed by a second incubation for a further 1 h in a mixture of 50% formamide and 20% PEG. This was followed by an extended third incubation with a solution of 50% formamide and 20% PEG for 6 h. Samples were stored in the final mixture at 4°C until assayed. Samples without addition of primary antibody were used as negative controls. Images shown are representative of independent triplicates.

Samples were observed using an inverted Eclipse Ti inverted microscope (Nikon France Instruments, Champigny sur Marne, France) equipped with a CSU-W1 spinning-disk (Yokogawa, Gataca Systems, France). The image was acquired thanks to a 40x oil objective CFI Plan Fluor NA 1.30 (voxel size 275 × 275 × 500nm), in combination with sCMOS Prime 95B camera (Photometrics, UK). All the devices are piloted by MetaMorph (Molecular DEVICES, Etats-Unis). Images were processed using ImageJ (Schindelin et al. 2012) for maximum intensity projection and rescaling of cropped images.

Flow cytometry of macrophages and tumoroids

The Live Dead Near viability staining kit (633 nm, InvitrogenTM) was used to determine the viability of macrophages after thawing and detachment by flow cytometry. Cells were labeled with the Live Dead Near viability staining kit (633 nm, InvitrogenTM), washed and fixed with 4% paraformaldehyde (PFA). The amount of live cells was compared between conditions.

In addition, the amount of primary macrophages in the three co-culture models was determined by flow cytometry based on CD11b positive expression (Figure S6A). For this, the co-culture models were first double digested as described above to obtain single cells, and then labeled with 1μg of mouse anti-CD11b antibody conjugated to BV605 (BD, Biosciences) for 30 min at room temperature in the dark.

Furthermore, for the phenotyping of macrophages post-co-culture with tumoroids in the three models, the co-culture models were first double-digested as described above to obtain single cells. Subsequently, they were labeled with the following antibodies: BV605-conjugated anti-human CD11b, Pe-Cy5-conjugated anti-human CD80, BV786-conjugated anti-human CD86, Pe-Cy7-conjugated anti-human HLA-DR, PE-conjugated anti-human CD206, and BV421-conjugated anti-human CD163 (BD, Biosciences) (Figure S6B). For all the flow cytometry analysis experiments, the samples were then washed and fixed with 4% PFA.

Cell sorting by flow cytometry after co-culture

After 96 h of coculture of primary macrophages with tumoroids, the three models were trypsinized and sorted by flow cytometry. Primary macrophages post-culture were selected using the GFP fluorescence bandpass filter at 525/50 nm with a 488 nm laser 278 on an SH800 cell sorter (Sony, Inc).

Total protein extraction

Total protein extraction of the primary macrophages, isolated by flow cytometry, was conducted using RIPA buffer (150 mM NaCl, 50 mM Tris, 5 mM EGTA, 2 mM EDTA, 100 mM NaF, 10 mM sodium pyrophosphate, 1% NP40, 1 mM PMSF, and 1X protease inhibitors). The extraction involved three rounds of 30-s sonication at 50% amplitude on ice, followed by centrifugation (16,000 × g, 10 min, 4°C) to remove cell debris. The resulting supernatants were collected, and the protein concentrations were determined using a Bio-Rad Protein Assay Kit as per the manufacturer's instructions. To standardize the protein quantities between macrophage samples, 20 μg of each of protein sample was used for digestion and subsequent shotgun proteomics analysis.

Shotgun proteomics

Protein digestion was carried out using the FASP method.[38] Initially, the sample was treated with a reduction solution containing 100 mM DTT in 8 M urea in 0.1 M Tris/HCl, pH 8.5 (UA buffer) and incubated for 15 min at 95°C. Subsequently, the protein solution was loaded onto 10 kDa Amicon filters, followed by the addition of 200 μL of UA buffer and centrifugation for 30 min at 14,000 g. Subsequently, 200 μL of UA buffer was added to the filter and centrifuged for another 30 min at 14,000 g. Next, 100 μL of alkylation solution (0.05 M iodoacetamide in UA buffer) was applied and incubated for 20 min in the dark, followed by centrifugation for 30 min at 14,000 g. Afterward, a 50 mM ammonium bicarbonate solution (AB) was added and centrifuged again for 30 min at 14,000 g. This step was repeated three time. For the digestion process, 50 μL LysC/Trypsin at 20 μg/mL in AB buffer was added and incubated at 37°C overnight. The digested peptides were recovered after centrifugation for 30 min at 14,000 g. Then, two washes with 100 μL of AB buffer were performed by centrifugation for 30 min at 14,000 g. Finally, the eluted peptides were acidified with 10 μL of 0.1% trifluoroacetic acid (TFA) and dried under vacuum.

LC-MS/MS analysis

The dried samples were reconstituted in 20 μL of a 0.1% TFA solution and 5 μL of sample was desalted using an Evotip Pure (Evosep, Odense, Denmark). Then, the peptides was separated and analyzed by Evosep One LC system coupled to a timsTOF Flex (Bruker

Daltonics, Germany) mass spectrometer. The Evosep One system operated with 60 Samples Per Day (60 SPD) method using an 8 cm × 150 μm reverse-phase column maintained at 40°C. Analytical columns were connected using a fused silica ID emitter (10 μm ID; Bruker Daltonics) within a Captive spray source (Bruker). Samples were acquired in DIA-PASEF mode, with spectra acquired within an m/z range of 100–1700 and an Ion Mobility range from 1.51 to 0.6 V cm−2.

MALDI mass spectrometry imaging of co-cultured tumoroids (MALDI-MSI)

The solid co-culture models were analyzed by Matrix-Assisted Laser Desorption/Ionization (MALDI) mass spectrometry imaging. The models were fixed in a solution of 2% paraformaldehyde with 0.1% glutaraldehyde in PBS for 24 h, then embedded in gelatin and frozen at −80°C. The tumoroids were then sectioned at 16 μm using a Leica cryostat (Leica Microsystems, Nanterre, France). The tumoroid sections were then placed on ITO-coated glass slides (LaserBio Labs, Valbonne, France) and placed in a vacuum desiccator for 15 min before matrix application. The matrix was applied by sublimation, for which 300 mg of DHB (2,5-dihydroxybenzoic acid) was weighed and spread on a 10 cm^3 glass plate. An oil bath ( ) adapted to the dimensions of the Ace vacuum sublimation apparatus (Sigma, France) was used to heat only the bottom of the chamber. The heating bath was equipped with a display to control the temperature (between 25°C and 225°C), where a temperature of 150°C was set. The ITO glass slide containing the tissue section was fixed to the inside of the sublimation system with a thermally conductive slide underneath. The size of the thermally conductive slide is the same as the ITO glass slides. The sublimation chamber was sealed with the CAPFE O-ring metal clamp and connected to the suction pump to create an internal vacuum. It was allowed to reach stability for 5 min. The upper contents were then filled with ice and the system allowed to cool for a further 5 min. Finally, the sublimation chamber was placed in a heating bath for the sublimation process for 10 min. After this time, the chamber was removed from the heating bath and allowed to cool at room temperature for 5 min. After this cooling period, the vacuum pump was switched off and the pressure was slowly released by gently loosening the tube connected to the sublimation chamber. This procedure resulted in the acquisition of a uniform matrix layer. The MALDI mass spectrometry images were performed on a RapifleX Tissuetyper MALDI TOF/TOF instrument (Bruker Daltonics, Germany) equipped with a smartbeam 3D laser. The MSI mass spectra were acquired in the positive delayed extraction reflectron mode using the 500–1300 m/z range. Recorded spectra were averaged from 200 laser shots per pixel, using a 10μm spatial resolution raster. Mass spectra were acquired using FlexControl (version 4.0, Bruker Daltonics) and MALDI-MSI data were processed and analyzed using SCiLS Lab software (SCiLS Lab 2019, SCiLS GmbH). Standard processing techniques for MALDI-MSI were applied, including baseline removal using a convolution method and data normalization using the Total Ion Count (TIC) method.[39,40] The pre-processed data were then clustered using the bisecting k-means algorithm to achieve spatial segmentation.[41] This involved first applying separate segmentation to each tissue and then clustering all tissue data together for global segmentation. Spatial segmentation involved grouping spectra based on their similarity using a clustering algorithm, with pixels in the same cluster being color coded. Edge-preserving image denoising was applied to reduce pixel-to-pixel variability. It is important to note that the color assigned to a cluster is arbitrary and several unrelated regions may share the same color, indicating similar molecular content. The segmentation results were visualized on a dendrogram resulting from hierarchical clustering. Branches on the dendrogram were determined by calculating the distance between each cluster. By selecting different branches on the dendrogram, a segmentation map was generated in which regions with different molecular composition were highlighted by different color coding.

Tumoroid response to paclitaxel

The semi-liquid model was used to analyze the pharmacological response of tumoroids compared to tumoroids co-cultured with macrophages. Tumoroids were cultured in 100 μL of complete medium containing 2% Matrigel at a density of 100,000 tumoroid cells with or without 30,000 macrophages per well in a 96-well plate coated with 1.5% agarose. Tumoroids were allowed to develop for 72 h and then treated with paclitaxel for 7 days before viability assessment. Cell viability was assessed using CellTiter-Glo 3D (Promega) according to the manufacturer's instructions, with results standardized against controls. Paclitaxel concentrations varied from 0.01 μmol to 100 μmol (8 concentrations) and DMSO controls were included. After 7 days, 100 μL of CellTiter-Glo3D reagent (Promega, Madison, WI, USA) was added to each well. The plate was mixed for 25 min at room temperature and luminescence was measured using a TriStar2 S LB 942 Multimode Microplate Reader.

Quantification and statistical analysis

For all flow cytometry analysis experiments, the samples were analyzed using CytoFLEX LX 2020 (Beckman Coulter), and the flow cytometry data were processed using KALUZA software. Data are presented as mean ± standard error in triplicate. Statistical significance between conditions was calculated using a t-test with multiple comparisons. Significance levels were denoted as follows: ****$p < 0.0001$; ***$p < 0.001$; **$p < 0.01$; *$p < 0.05$; NS, not significant.

Proteomics data analysis for all DIA files was conducted using DIA-NN software. A search against the human UniProt reviewed Homo sapiens database (downloaded in May, 2023, 20,422 entries) was performed using library-free workflow. A maximum of 2 trypsin missed cleavages were allowed and the maximum variable modification was set to 3. Carbamidomethylation (Cys) was set as the fixed modification, whereas methionine oxidation was set as variable modification. The peptide length range was set to 7–30 amino acids, precursor charge range 1–4, precursor m/z range 100–1700, and fragment ion m/z range 200–1700. False discovery rates (FDRs) at the protein and peptide level were set to 1%. Match between runs was allowed. Analysis of the identified proteins

was performed using Perseus (version 1.6.15.0) software.[42,43] Statistical tests were performed using a t-test test with a *p*-value of 5% while preserving grouping in randomization. Visual representation of significant protein variations was obtained using hierarchical clustering analysis in the form of a heatmap. Gene ontology analysis, including cellular components and biological processes, was performed using the FunRich 3.0 analysis tool.[44]

Tumoroid response to paclitaxel was analyzed using GraphPad Prism 6, with non-linear regression to generate response curves and IC-50 values.